ΣΧΟΛΗ ΜΗΧΑΝΙΚΩΝ
Τμ. ΜΗΧΑΝΙΚΩΝ ΒΙΟΜΗΧΑΝΙΚΗΣ ΣΧΕΔΙΑΣΗΣ ΚΑΙ ΠΑΡΑΓΩΓΗΣ
Π.Μ.Σ. «ΜΗ ΕΠΑΝΔΡΩΜΕΝΑ ΑΥΤΟΝΟΜΑ ΚΑΙ ΤΗΛΕΚΑΤΕΥΘΥΝΟΜΕΝΑ ΣΥΣΤΗΜΑΤΑ»

ΠΡΟΓΡΑΜΜΑ ΜΕΤΑΠΤΥΧΙΑΚΩΝ ΣΠΟΥΔΩΝ

«ΜΗ ΕΠΑΝΔΡΩΜΕΝΑ ΑΥΤΟΝΟΜΑ ΚΑΙ ΤΗΛΕΚΑΤΕΥΘΥΝΟΜΕΝΑ ΣΥΣΤΗΜΑΤΑ»

ΤΙΤΛΟΣ:

A FUZZY LOGIC-BASED APPROACH FOR PRECISE UAV SHIP DECK LANDINGS

Ονοματεπώνυμο Σπουδαστή:

ΤΣΙΤΣΕΣ ΙΩΑΝΝΗΣ

Ονοματεπώνυμο Υπεύθυνου Καθηγητή:

ΖΑΧΑΡΙΑ ΠΑΡΑΣΚΕΥΗ

ΔΙΑΤΡΙΒΗ

ΦΕΒΡΟΥΑΡΙΟΣ 2024

Μέλη Εξεταστικής Επιτροπής

Ζαχαριά Παρασκευή

Paraskevi Zacharia
Digitally signed by Paraskevi Zacharia
Date: 2024.06.08 19:51:42 +03'00'

Παπουτσιδάκης Μιχαήλ

Digitally signed by ΜΙΧΑΗΛ ΠΑΠΟΥΤΣΙΔΑΚΗΣ
Date: 2024.06.16 20:27:47 +03'00'

Χατζόπουλος Αβραάμ

Digitally signed by AVRAAM CHATZOPOULOS
Date: 2024.06.13 16:39:31 +03'00'

ΔΗΛΩΣΗ ΣΥΓΓΡΑΦΕΑ ΜΕΤΑΠΤΥΧΙΑΚΗΣ ΕΡΓΑΣΙΑΣ

Ο κάτωθι υπογεγραμμένος Ιωάννης Τσιτσές του Πέτρου-Σπυρίδωνος, με αριθμό μητρώου 8096626 φοιτητής του Προγράμματος Μεταπτυχιακών Σπουδών «Μη Επανδρωμένα Αυτόνομα και Τηλεκατευθυνόμενα Συστήματα» του Τμήματος Μηχανικών Βιομηχανικής Σχεδίασης και Παραγωγής της Σχολής Μηχανικών Πανεπιστημίου Δυτικής Αττικής, δηλώνω υπεύθυνα ότι: «Είμαι συγγραφέας αυτής της μεταπτυχιακής εργασίας και ότι κάθε βοήθεια την οποία είχα για την προετοιμασία της είναι πλήρως αναγνωρισμένη και αναφέρεται στην εργασία. Επίσης, οι όποιες πηγές από τις οποίες έκανα χρήση δεδομένων, ιδεών ή λέξεων, είτε ακριβώς είτε παραφρασμένες, αναφέρονται στο σύνολό τους, με πλήρη αναφορά στους συγγραφείς, τον εκδοτικό οίκο ή το περιοδικό, συμπεριλαμβανομένων και των πηγών που ενδεχομένως χρησιμοποιήθηκαν από το διαδίκτυο. Επίσης, βεβαιώνω ότι αυτή η εργασία έχει συγγραφεί από μένα αποκλειστικά και αποτελεί προϊόν πνευματικής ιδιοκτησίας τόσο δικής μου, όσο και του Ιδρύματος.
Παράβαση της ανωτέρω ακαδημαϊκής μου ευθύνης αποτελεί ουσιώδη λόγο για την ανάκληση του διπλώματός μου».

Ο δηλών
Ιωάννης Τσιτσές

Ημερομηνία
20/02/2024

A Fuzzy Logic-Based Approach for Precise UAV Ship Deck Landings

ΤΣΙΤΣΕΣ ΙΩΑΝΝΗΣ

Μεταπτυχιακή Διατριβή που υποβάλλεται στο καθηγητικό σώμα για την μερική εκπλήρωση των υποχρεώσεων απόκτησης του μεταπτυχιακού τίτλου του Προγράμματος Μεταπτυχιακών Σπουδών «Μη Επανδρωμένα Αυτόνομα και Τηλεκατευθυνόμενα Συστήματα» του Τμήματος Μηχανικών Βιομηχανικής Σχεδίασης και Παραγωγής του Πανεπιστημίου Δυτικής Αττικής

Abstract
This paper introduces a fuzzy logic-based autonomous ship deck landing system for fixed-wing unmanned aerial vehicles (UAVs). The ship is assumed to maintain a constant course and speed. The aim of this fuzzy logic landing model is to simplify the task of landing UAVs on moving ships in challenging maritime conditions, relieving operators from this demanding task. The designed UAV ship deck landing model is based on a fuzzy logic system (FLS), which comprises three interconnected subsystems (speed, lateral motion, and altitude components). Each subsystem consists of three inputs and one output incorporating various fuzzy rules to account for external factors during ship deck landings. Specifically, the FLS receives five inputs: the range from the deck, the relative wind direction and speed, the airspeed, and the UAV's flight altitude. The FLS outputs provide data on the speed of the UAV relative to the ship's velocity, the bank angle (BA), and the angle of descent (AOD) of the UAV. The performance of the designed intelligent ship deck landing system was evaluated using the standard configuration of MATLAB Fuzzy Toolbox.

Keywords
UAV ● Autonomous Ship-Deck Landing System ● Fuzzy Logic System ● MATLAB Fuzzy Toolbox

Contents

Figures

Tables

List of Acronyms

AAW	→	Azimuth Angle of Wind
AOD	→	Angle Of Descent
BA	→	Bank Angle
BDA	→	Battle Damage Assessment
COG	→	Course Over Ground
COTS	→	Commercial Off-The-Shelf
CR	→	Corner Reflector
EMO	→	Electronic Magnetic Operations
EW	→	Electronic Warfare
FLS	→	Fuzzy Logic System
GPS	→	Global Positioning System
IAS	→	Indicated airspeed
INS	→	Inertial Navigation System
ISTAR	→	Intelligence – Surveillance - Targeting– Reconnaissance
LOS	→	Line Of Sight
NLOS	→	No Line Of Sight
RLD	→	Range from Landing Deck
RCS	→	Radar Cross-Section
RF	→	Radio Frequency
RFID	→	Radio Frequency Identification
RSD	→	Relative Speed of the Drone
RWS	→	Relative Wind Speed
SAR	→	Search And Rescue
SOG	→	Speed Over Ground
TDOA	→	Time Difference of Arrival
UAV	→	Unmanned Aerial Vehicle
UHF	→	Ultra-High Frequency
UNCLOS	→	United Nations Convention on the Law of the Sea
WS	→	Wind Speed

1. Introduction

1.1 Importance of UAVs in the Maritime Domain

Nowadays, the utilization of drones in the maritime domain is rapidly increasing. Their use for civil missions, as well as military operations vary greatly. Regarding the civil sector, from transporting spare parts, documents, medicine, etc. between land and ships at sea or between ships at sea only [1], to controlling traffic and the emission of pollutants from ships or even preventing illegal activities such as piracy, smuggling and illegal fishing [2], drones – and especially Unmanned Aerial Vehicles (UAVs) - are used. The underlying reason for this fact lies in the drone's numerous sensing capabilities and interchangeable payload equipment [3], combined with the reduced risk, time and cost that the UAVs provide in a wide range of missions [1]. Additionally, drones are used for "3D" missions, meaning operations too "dull, dirty, or dangerous" for humans in military or government applications, such as water ballast tank or cargo inspections, hull or damage surveys after an accident or other forms of inspections in toxic and remote spaces [1].

On the other hand, in the military/security domain, another vast range of missions is covered solely from UAVs, both in peacetime and in wartime periods. Drones, for example, provide unparalleled surveillance capabilities for border security, facilitating real-time monitoring of large areas with minimal risk to individuals on the ground, combining also the ability to deploy easily and respond immediately to any potential threat or emergency [2]. Furthermore, drones are used for Search And Rescue (SAR) missions, improving response times and limiting exposure to dangerous conditions or even by dropping flotation devices for lifeguarding purposes [3]. Additionally, UAVs are mostly used in maritime surveillance operations, actively monitoring and tracking ships, boats, and various vessels to uphold the safety and security of maritime traffic, while concurrently thwarting illicit activities including smuggling, piracy, and illegal fishing or even facing hostile counterparts violating the United Nations Convention on the Law of the Sea (UNCLOS). UAVs are also used as moving targets during military exercises of naval forces.

Lastly, in wartime, the operation capabilities of modern maritime military UAVs experience further augmentation. Depending on the payload and the equipment of the UAV, a drone is able to undertake missions such as: Battle Damage Assessment (BDA), Intelligence – Surveillance - Targeting– Reconnaissance (ISTAR), Electronic Magnetic Operations (EMO), tactical spoofing, rocket and missile launching, as well as countermeasures launching. Recognizing the value of utilizing UAVs in the maritime domain, the US Navy, as well as the UK Royal Navy [1], have integrated a variety of different drones in their arsenal, leading the way in modern warfare and naval research technology.

1.2 Autonomous Landing System

Concerning the operation of UAVs, an abundance of literature exists that describes autonomous flight navigation. However, landing, one of the most critical parts in the flight of a drone, is a topic seriously neglected by the academic community. Even today, most UAV landings are performed manually by their operators, from inside the drone's ground station, depriving the drone pilot of the peripheral vision, the instinctive senses and the space perception during the procedure. As a result, the majority of UAV's crashes happen due to human errors, during take offs and landings, which constitute the most dangerous parts of a drone's flight [4].

More specifically, during ship-deck landings, the difficulty of manually guiding the UAV to touchdown, increases exponentially, demanding even more experience and skill from the drone pilot. The unpredictable nature of the maritime environment, characterized by low visibility, strong wings, high humidity and noticeable waves, in combination with the dynamic motion of the landing platform of the ship in the sea with its limited dimensions, pose a great, sometimes even impossible, challenge for the drone pilot. Consequently, the imperative arises for the development of an autonomous landing system, crucially contributing to the progression of drone technology within the maritime sector.

This paper focuses on the concluding stages of UAV operations, specifically the final approach and touch-down periods. It introduces a fuzzy logic-based autonomous ship-deck landing system for fixed-wing UAVs as a proposed solution to most of the complex problems mentioned earlier.

1.3 Electronic Warfare Resistant Landing

Additionally, a noteworthy consideration in this study involves ensuring the Electronic Warfare (EW) Resistance of the fuzzy logic-based autonomous ship-deck landing system, particularly in military applications in order to guide the UAV in a safe and successful landing under a harsh and dense electromagnetic environment. The Global Positioning System (GPS) stands as an important component within the equipment on a UAV, serving as a sophisticated localization mechanism. Its primary function is to provide the drone with vital data regarding its precise position, speed, and height level. However, this pivotal, for the drone, system is susceptible to spoofing and jamming [5]. Lessons learned from the Israel-Hamas conflict prove that EW and more specifically GPS jamming, affects all kinds of civil GPSs, and consequently, counters the drone attacks from Hezbollah and Hamas [6]. Considering that civil GPSs are utilized much more frequently than military GPS units in UAVs due to their cost, it easily understandable that the vulnerability of the autonomous UAV systems, is real. In the Ukraine – Russian War, EW technics, such as jamming and spoofing, are utilized from the Russian Army to take down Ukrainian UAVs [7]. To counter these modern warfare operational tactics, this paper proposes the integration of Inertial Navigation System (INS) sensors with altimeters, anemometers, TDOA based localization systems and more equipment onboard UAVs. This integration aims to enhance the estimation of the vehicle state and position, even in a hostile electromagnetic environment.

2. Definitions and Terminology

This chapter introduces fundamental terms related to the autonomous ship-deck landing system based on fuzzy logic, providing a comprehensive clarification of essential concepts and information.

2.1 Indicated Airspeed

Indicated airspeed (IAS) is the speed of the UAV relative to the body of air through which it is flying [8]. It is measured using an airspeed sensor and it is expressed in knots. In other terms, the IAS is "*the speed of an aircraft as shown on its pitot static airspeed indicator, calibrated to reflect standard atmosphere adiabatic compressible flow at sea level, uncorrected for airspeed system errors"* [9]. Basically, IAS represents the dynamic pressure upon the airspeed sensor, as the aircraft moves through a body of air. It is a function of the dynamic pressure experienced by the UAV and the atmospheric density of air surrounding the drone in a certain altitude. In practice, however, we consider that air density is independent of the attitude due to the very low heights (during the whole landing process maximum height is 330 ft - around 100m). As a result, air density is considered to be constant, so there is no need for a dynamic pressure sensor to compute airspeed [5].

IAS is the most important speed of the pilot from an aerodynamic point of view, especially when controlling the aircraft during take-offs or landings. It differs completely from the ground speed, which is the actual aircraft speed in relations to the ground. For fixed-wing aircrafts, such as the UAVs studied in this work, it is the IAS that guarantees lift - not ground speed. So, for example, if airspeed is minimum, then stability conditions are severe and the maneuvering abilities are limited [4].

2.2 Azimuth Angle of Wind and Relative Wind Speed

The Azimuth Angle of Wind (AAW) is the direction from which they wind is blowing, measured in degrees clockwise from North on an azimuth circle. An azimuth circle consists of 360 degrees. Traditionally, wind direction is reported as one of eight compass points (N, NE, E, SE, S, SW, W, NW) [10], which depicts certain degrees in the azimuth circle as shown in the table below:

Table 1:The Eight Compass Points of the Azimuth Circle

Compass Point	Degrees in the Azimuth Circle	Radians in the Azimuth Circle
North (N)	0 or 360	0 or 2pi
North - East (NE)	45	pi/4
East (E)	90	pi/2
South - East (SE)	135	3pi/4
South (S)	180	pi
South – West (SW)	225	5pi/4
West (W)	270	3p/2
North – West (NW)	315	7pi/4

The AAW is either True or Relative depending on the North used as a reference. True North corresponds to the direction indicated by a gyroscopic compass and is represented on a map as the line of longitude which converging on the North Pole [11]. When the True North is used for the Azimuth Angle of Wind, it leads to the calculation of the True Wind. Conversely, Relative Wind is calculated using a Relative North as a reference (Figure 1). In the case of a fixed-wing UAV, the Relative North is the nose of the UAV. Consequently, the Relative AAW signifies the wind direction relative to the UAV. In the FLS later, we utilize only the Relative AAW.

The WS [12], is the speed of the wind. WS is also separated into True WS and Relative WS. True WS (Ground Wind), "*is the actual speed of the wind as it passes over land or the surface of the sea*" [12]. Relative or Apparent Wind Speed (RWS) is the wind that a body (aircraft, UAV, ship etc) "feels" as it moves through space. The AAW as well as the WS are measured by an anemometer. Initially, the anemometer measures the relative values of the two variables and then, with the known course and speed of the vehicle, it calculates the true values. For example, if there is a wind of 10 knots from one direction, the anemometer of a stationary UAV will calculate 10 knots relative and true WS. However, if the UAV starts moving towards the direction of the wind with 80 knots, then the RWS that will "ram" the body of the UAV and will be calculated by the anemometer is going to be 90 knots.

Figure 1: Wind Calculator App

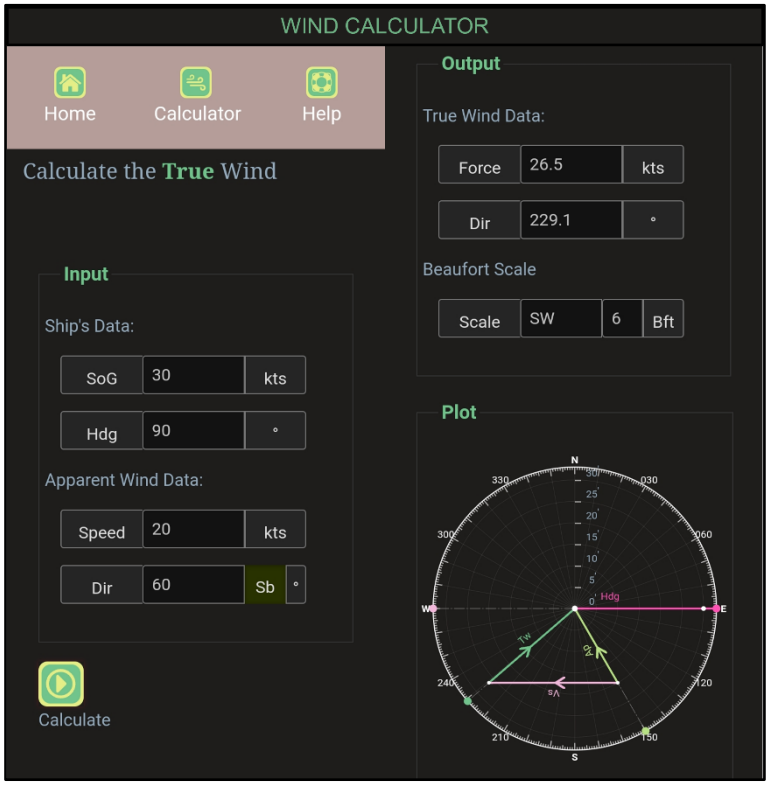

2.3 Range from Landing Deck

The range of the UAV from the landing deck of the ship (RLD) is measured in meters by a Time Difference Of Arrival (TDOA) based localization mechanism. The working principle of the TDOA system is as follows: A modulated signal is transmitted from the UAV and this signal is captured at three or more probes placed in different locations around the landing deck. Then, the signal captured at each receiver is shifted in time to locate a position of maximum correlation and this time delay is later multiplied by the speed of light, calculating the distance difference between each probe. Afterwards, the distance difference is plotted as a set of hyperbolic lines between the pairs of the probes (Figure 3) and lastly the intersection of the lines indicates the location of the emitting drone [13].

In order to calculate the distance of the drone from the ship, the exact position of the UAV in the 2D plane is required (Figure 4). Achieving this localization requires the implementation of a 3-node TDOA based system. In the context of this paper, however, a four-node TDOA system is employed to pinpoint the UAV within three-dimensional space. This configuration allows for the determination of both the RLD and altitude of the UAV, as elaborated upon in subsequent sections.

Furthermore, since the times of arrival of the signal are measured by different receivers in the TDOA based localization mechanism, precise synchronization between all these nodes is essential [14]. Also, TDOA is vulnerable to the time-delay caused by No Line Of Sight (NLOS) path, as the system's measurements are based on the assumption that the signal travels the shortest path, or else along the Line Of Sight (LOS), from the source (the emitting UAV) to the receiver (node) [15].

Figure 2: The TDOA based localization four-node system

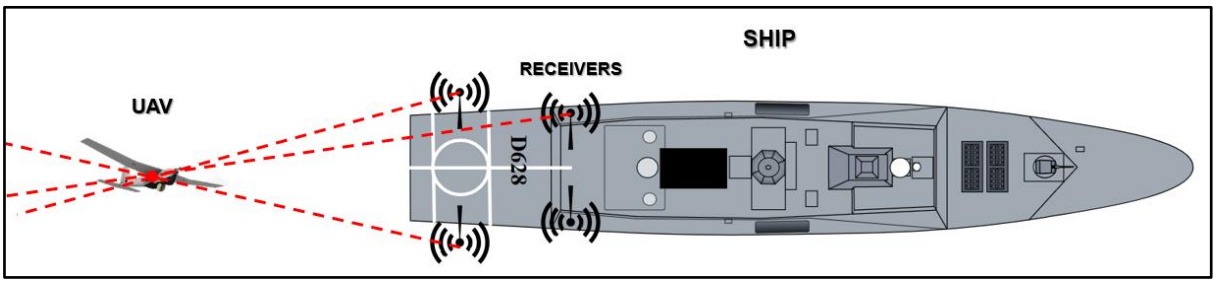

Figure 3: A TDOA based localization mechanism with two nodes

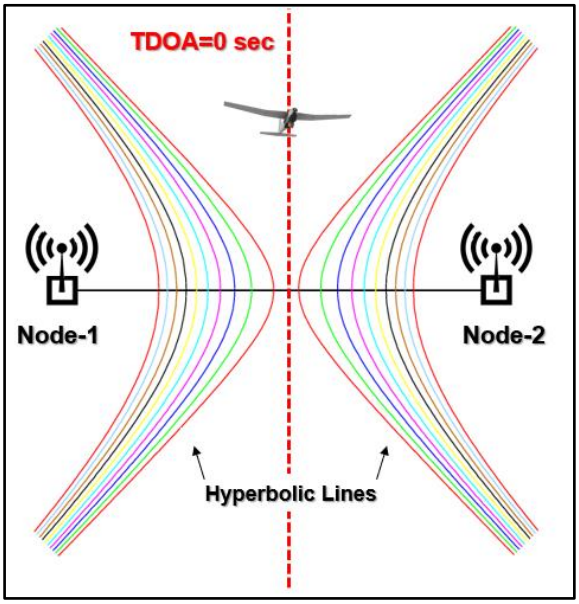

Figure 4: TDOA based three-node system to calculate the distance of the UAV in two-dimensional space.

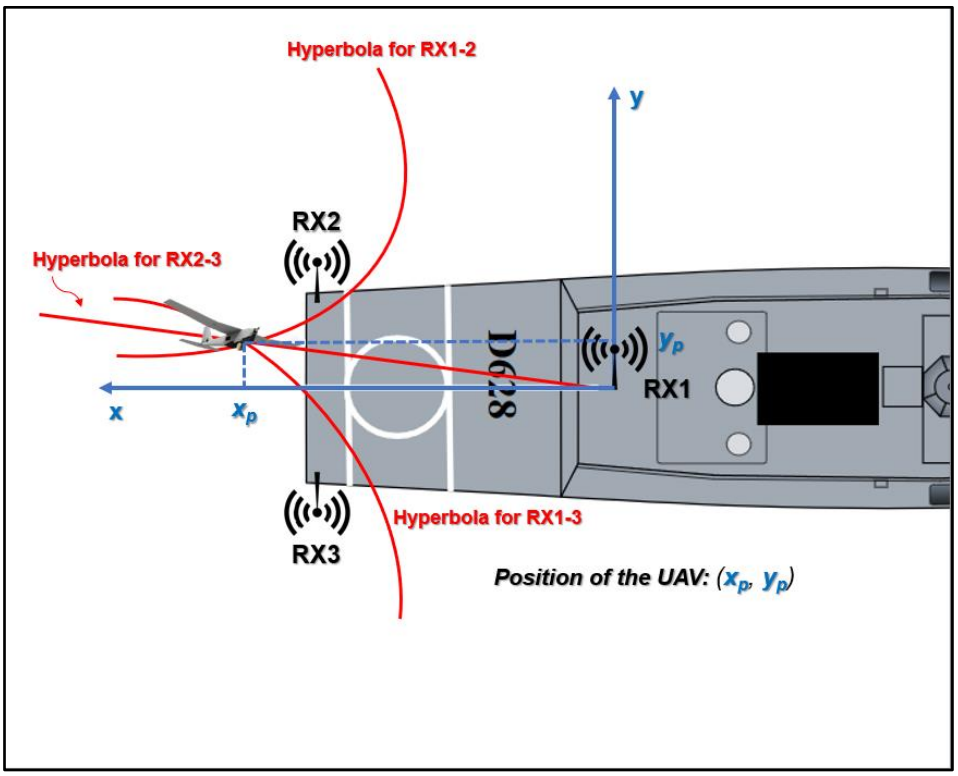

2.4 Altitude

The altitude of the UAV is the distance from the surface of the sea. It is measured in feet (ft) by a barometric altimeter, which measures atmospheric pressure to estimate altitude. However, weather conditions can affect atmospheric pressure and that is why altimeters are often calibrated at the takeoff site. Also, to increase the accuracy of the height value, a four-node TDOA based mechanism is utilized [16], providing the position of the UAV in 3D space, during the entire phase of the landing.

2.5 Relative Speed of the Drone

The Relative Speed of the Drone (RSD) is the speed of the UAV in reference with the speed of the ship. More specifically, during the landing phase, it represents the difference between the Speed Over Ground (SOG) of the UAV and the SOG of the Ship, as the UAV approaches the landing deck of the ship, measured in knots. In the context of this paper, where the ship moves in front of the drone, it is calculated by subtracting the constant SOG of the ship from the SOG of the UAV.

2.6 Bank Angle

The Bank Angle (BA) is the angle of turn in the azimuth plane of an aircraft and is measured in degrees (°) [17]. In other terms, it is the angle between the aircraft's normal, or vertical, axis and the earth's vertical plane containing the aircraft's longitudinal axis. The BA of an aircraft is measured from 0° to 179° port or starboard (left or right) [18]. When an aircraft makes a turn, it banks to one side, and the bank angle is the amount by which the aircraft is tilted. It is dependent on the forces of lift and weight that are acted upon the UAV.

2.7 Angle of Descent

The Angle of Descent (AOD) is the angle between the aircraft's horizontal axis and the earth's horizontal plane. It indicates how steep the “dive” of the aircraft is during the landing or the take-off phase and it is measured in degrees.

3. Autonomous Ship-Deck Landing System

3.1 Ship Characteristics and Sensors

For the purpose of this paper, we consider the ship's COG and speed over ground (COG & SOG) to be constant during the landing phase of the drone. Due to the limited dimensions of the helidecks on most ships, the most successful landing of a fixed-wing UAV would involve the use of a vertical rope or a net to "catch" the flying drone. In this context, "SkyHook" [19] is proposed as a capture system onboard the helideck of the ship (Figure 5), with indicative dimensions as follows: Length: 8.8m, Width: 5.3m, Height: 17.67m. Also, we consider the height level of the ship's landing deck from sea surface to be 8 meters, a number that is needed later (Figure 6).

Additionally, four, spatially-separated, nodes of the TDOA based localization mechanism are planted in different positions on the landing deck in order to track the UAV's position in the three-dimensional space during its approach to the ship [20]. The ultimate goal of the autonomous landing system is to present an alternative navigation approach, that operates independently of GPS, providing a robust and self-reliant solution in a contested electromagnetic environment.

For even better accuracy and precision during the last phase of the landing procedure, in a RLD less than 20 meters, the use of a passive Ultra High Frequency (UHF) Radio Frequency Identification (RFID) based UAV positioning system is proposed [14]. The best candidate RFID for this role, is the MilliSign guidance system based on a batteryless tag to support UAVs in poor visibility and all-weather conditions [21]. A corner reflector (CR) array based chipless RFID tag and a one-shot slant range reading procedure with Commercial Off-The-Shelf (COTS) mmWave radar constitute the MilliSign system, as shown in Figure 7 below. The RFID tag is placed vertically in the longitudinal axis of the landing deck, right behind the receiver rope of the "Skyhook" capture system. This placement is designed to facilitate the alignment of the fixed-wing UAV with the "catch rope" in the final meters of its flight. (Figure 8). The chipless tag, measuring 292 mm x 600 mm x 19 mm and storing eight bits, is a conventional high radar cross-section (RCS) scatterer, with retro-reflective attributes for 3D incident wave and provides a wide 3D read range so that it can be read by the UAV's UHF radar from a distance of more than ten meters, with a viewing angle of more than 30 in elevation and azimuth. The tag is covered by a radome, as it is sensitive against debris such as dust, sand, mud, and water (rain), which can enter and deteriorate the backscattering RCS of the tag. The RFID Reader (mmWave radar), on the other hand, is deployed on the UAV and the communication between the reader and the tag is much more efficient in LOS.

Lastly, as a general observation, the majority of merchant ships encompassing bulk carriers, ferry ships, cargo ships etc. often cruise at eighteen to twenty-five knots. However, warships including destroyers, frigates or corvettes, are capable of operating at speeds approximately thirty-two knots. In this particular context, the designated maximum speed for the ship during the landing phase is stipulated as thirty knots. Subsequently, this value serves as the basis for determining the maximum RSD later.

Figure 5: SkyHook landing system.

Figure 6: Different Heights used for the Landing System

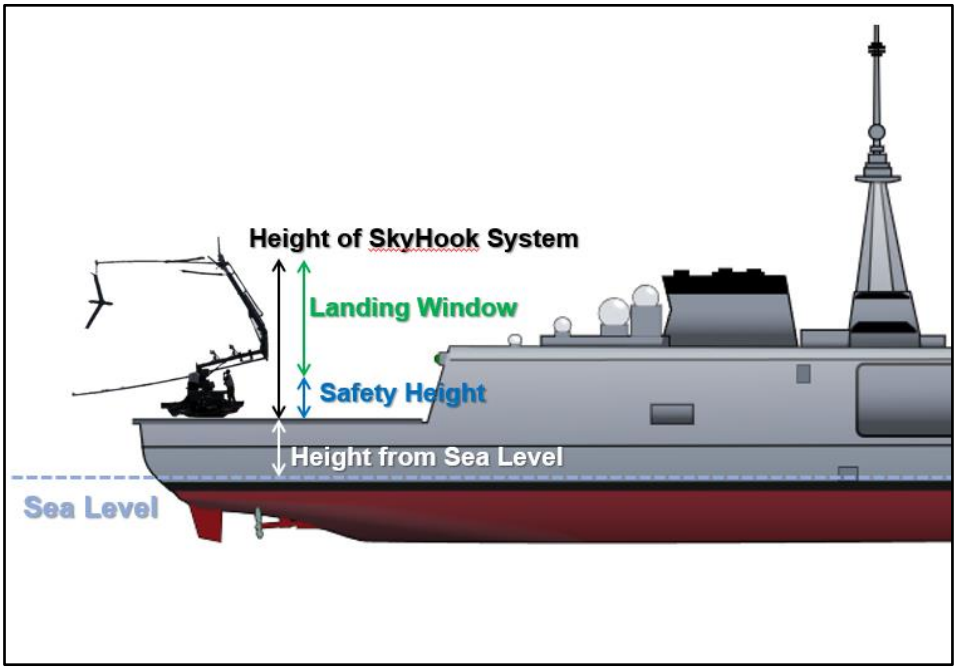

Figure 7: The chipless RFID tag used in the MilliSign System [20]

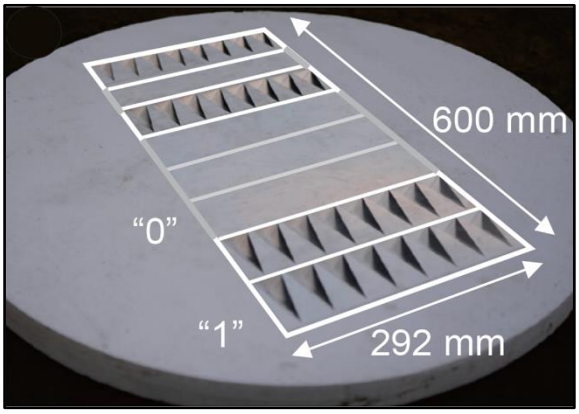

Figure 8: The chipless RFID tag on a tripod stand behind the SkyHook Landing System

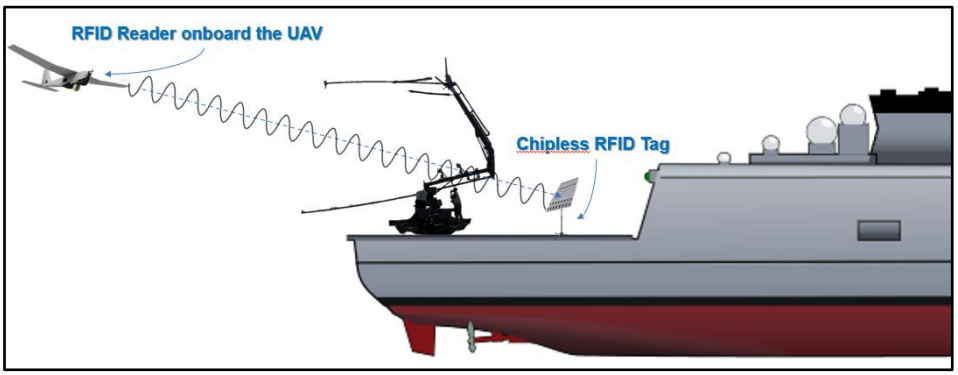

3.2 UAV Characteristics and Sensors

The fixed-wing UAV that is investigated in this paper, is a Small – Medium Size/Class drone (Figure 9), capable of reaching a maximum speed of 70 knots during the landing phase of its mission. Also, the BA of the UAV is considered to be a maximum of 60 degrees, indicative of a highly agile military UAV capable of executing sharp and steep turns. However, the ability of the UAV to turn at such degrees is immediately dependent on the IAS, which strongly affects the aerodynamics of the UAV.

Additionally, to enable precise landing, the UAV necessitates an array of sensors and equipment. The sensors of the fixed-wing UAV, are its "eyes" and "ears" that gather the information around the environment of the drone and send it to the "brain", or else, the microcontroller of the UAV. For the purpose of the autonomous ship-deck landing presented in this paper, the UAV is equipped with the following sensors:

- ✓ An Anemometer
- ✓ An Airspeed Sensor
- ✓ A Barometric Altimeter
- ✓ An Inertial Navigation System (INS)
- ✓ A Radio Frequency (RF) Transmitter for the TDOA based localization system
- ✓ A mmWave radar (RFID Reader)

Regarding the RFID Reader deployed on the UAV, its small size, lightweight design and cost effectiveness, as well as its minimal power requirements contribute to enhancing the UAV's autonomous capabilities [21].

Lastly, all these sensors constitute the essential equipment of a fixed-UAV to conduct a successful autonomous ship-deck landing as described in this work. The deliberate omission of a GPS sensor during the landing phase is driven by the necessity for the UAV to exhibit resistance against EW interference, as mentioned in the Introduction.

Figure 9: Examples of Small – Medium Size/Class UAVs

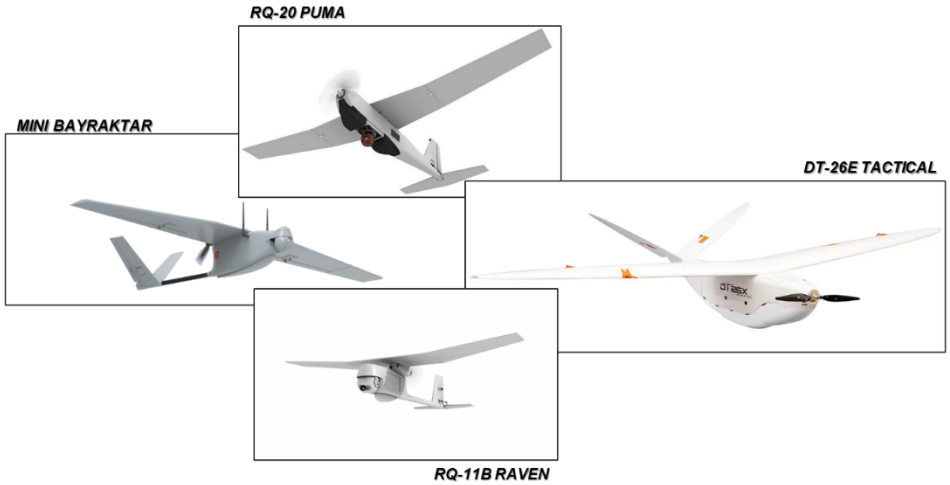

3.3 The Main Attributes of Landing

The scope of this paper is the design of a precise autonomous landing system utilizing fuzzy logic, in order to be used by fixed-wing UAVs during ship-deck landings. For a successful landing to take place, three variables must be taken into consideration [4]. First of all, the speed of the UAV is of the most importance and especially the RSD, in relation to the ship's SOG. The ship's data (COG & SOG) are inserted manually and sent to the UAV from the ground station, so that the drone is aware of the ship's fixed SOG and COG values. The UAV's relative speed indicates the rate at which it converges toward the ship's landing deck. Furthermore, for the effective operation of the landing system, the RSD must be a minimum of five knots, ensuring that the clips on the drone's wings can securely engage with the landing rope.

Secondly, the lateral position of the fixed-wing UAV with reference to the longitudinal axis of the deck of the ship is undeniably a noteworthy attribute during the landing phase of the drone. The scope of the landing system is to guide the UAV on the lateral middlepoint of the helideck, where the SkyHook's rope will be hanging, ready to "catch" the UAV. To achieve this part of the "outer loop" control [5], the BA of the UAV is modified, thereby modifying the angle of turn in the azimuth plane of the drone. In that way, the autonomous landing system guides the UAV along the desired trajectory rejecting external disturbances such as wind [5].

The final factor to be considered for a fixed-wing UAV during the execution of a landing on a ship's deck is the vertical position of the drone, expressed alternatively as its altitude. To reach the desired landing altitude, the UAV must "dive" gradually with a specific rate of descent. This is achieved by controlling the AOD of the fixed-wing drone. Nevertheless, for a successful landing, the UAV must maintain a minimum altitude of approximately 5 meters from the landing platform (13 meters from the sea surface) to mitigate the risk of the drone colliding with the helideck.

3.4 The Landing

The small-medium size fixed-wing UAV has completed its mission and is Returning To Base (RTB). When in range of the TDOA based UAV localization system, the drone takes its starting position 100 meters behind the ship, along the axis of equal distance, where the time difference of arrival and the difference in distance between three of the four nodes in the 2D x-y plane are zero (Figure 3). The short distance of 100 meters between the ship and the UAV when the landing phase begins is deliberately chosen so that smaller errors occur in the absence of a GPS [5]. At the same time, the data regarding the ship's constant SOG and COG are transferred via a telecommunication link to the UAV and the drone adjusts its own speed and course accordingly, utilizing the INS component. With the drone, now, following the landing path with the same course and speed as the ship, the landing phase begins as the fuzzy logic-based autonomous ship-deck landing system is enabled. During the approach of the UAV to the landing deck, the FLS controls the three main attributes of landing that are mentioned above in order to ensure a successful landing, against external factors such as the wind:

a) The RSD must always be greater than the velocity of the ship, so that it is able to approach the landing deck.
b) The lateral movement of the UAV needs to be mitigated by controlling the drone's BA to ensure that the UAV will follow the landing path.
c) The altitude of the UAV must decrease progressively by controlling the drone's angle of descent. This is essential to attain a specified height ranging between 5 to 15 meters above the landing deck (13 to 23 meters above the surface of the sea) facilitating the UAV's engagement with the "SkyHook" retrieval system's rope.

Around 20 meters from the capture rope, the MilliSign RFID guidance system is enabled and utilized in order to increase the precision of the autonomous landing system. The UAV then aligns with the batteryless chipless CR tag and navigates with pinpoint accuracy on the "SkyHook" system. Subsequently, at a relative speed exceeding 5 knots concerning the ship, the UAV maneuvers towards the landing rope and hooks on it.

4. Fuzzy Logic System and Methodology

Fuzzy logic "*is intended to model logical reasoning with vague or imprecise statements*" [11]. Fuzzy set theory provides a framework for dealing with classes of objects where the boundaries are not precisely defined. Instead of strict, absolute, binary membership (either true or false) [23], fuzzy sets allow for degrees of membership, acknowledging the gradual transition between the two aspects [22].

4.1 Input Data

To construct the fuzzy logic-based autonomous ship-deck landing system, five input variables are imported: the Indicated Airspeed, the AAW and the WS, the Altitude and the Horizontal Distance from the Landing Deck. The input data is received by the airspeed sensor, the anemometer, the barometric altimeter and the TDOA based localization system, respectively.

4.2 Output Data

Then, the fuzzy logic based autonomous landing system determines three output variables: the RSD, the AOD and the BA of the UAV by controlling the drone's throttle and ailerons. The FLS outputs, are determined by using the centroid method.

4.3 Type of Fuzzy Inference System

In the FLS, Mamdani fuzzy inference system is used. The reason for this choice lies in the output variables of the system [22]: In the Mamdani type, the output of each rule is a fuzzy set, in contrast with the Sugeno type that determines the output membership function as a constant or a linear value [22]. The RSD, the BA and the AOD of the fixed-wing UAV, as mentioned above, are defined as fuzzy sets.

4.4 Model Development

The fuzzy logic based autonomous ship-deck landing system utilizes the input data provided by the range of sensors in order to calculate the corrective maneuvers of the drone by using three fuzzy logic components. All fuzzy operations were made in Fuzzy Logic Toolbox of MATLAB using the "fuzzyLogicDesigner" command. The membership functions and rules employed, serving as encoded knowledge for predictions, were established through a heuristic technique. This means that the fuzzification process was executed practically without a guarantee to be optimal or rational, but is nevertheless sufficient for the scope of this paper. In Figure 10, the FIS Tree Plot is shown, with an overall presentation of the FLS.

Figure 10: The FIS Tree Plot

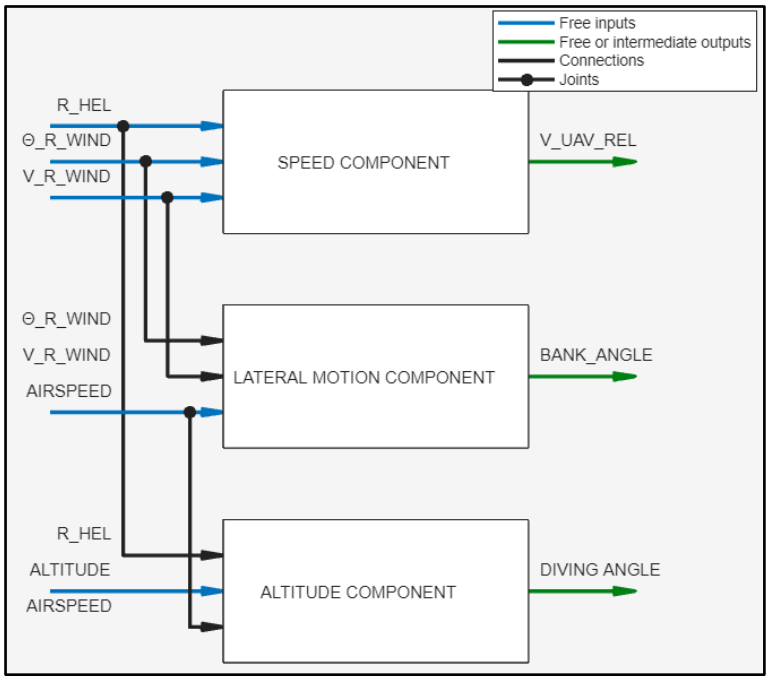

4.4.1 Speed Component

The first fuzzy logic subsystem block is the speed component, which is presented in Figure 11. The Mamdani Fuzzy Logic Component is used with three inputs: AAW, WS and RLD from the Landing Deck, and one output: the RSD with respect to the ship's velocity. The total number of rules is one hundred eighty-five (185) as shown in Figure 12.

Figure 11: The Speed Component

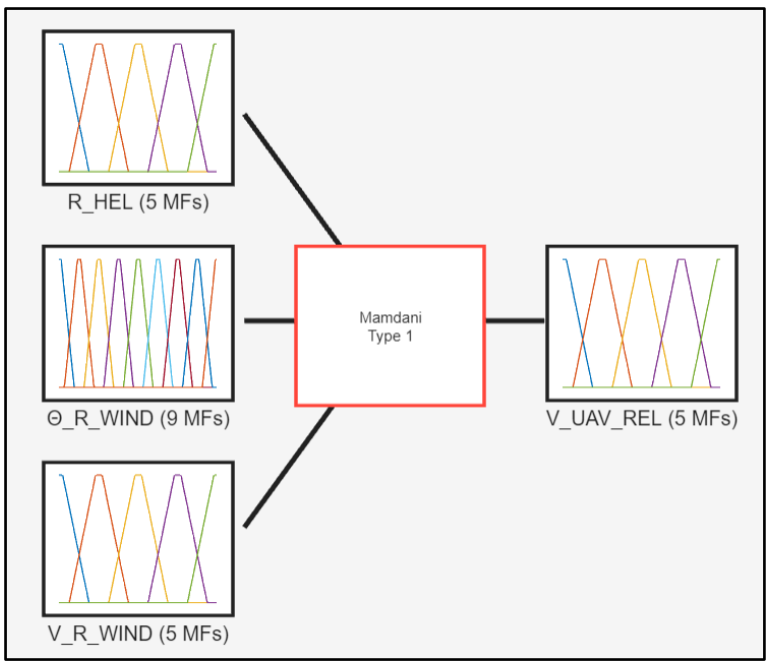

Figure 12: Rule Editor in the Speed Component

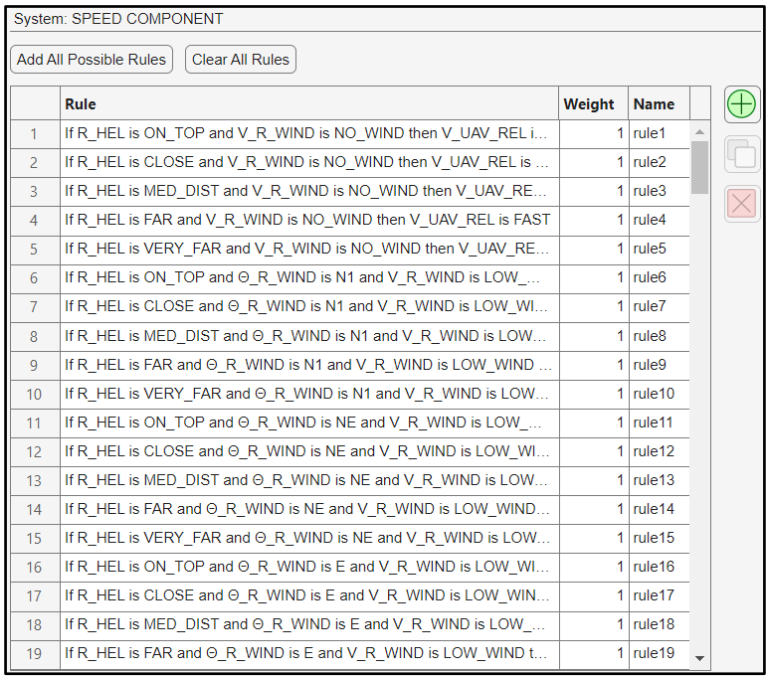

	Rule	Weight	Name
1	If R_HEL is ON_TOP and V_R_WIND is NO_WIND then V_UAV_REL i…	1	rule1
2	If R_HEL is CLOSE and V_R_WIND is NO_WIND then V_UAV_REL is …	1	rule2
3	If R_HEL is MED_DIST and V_R_WIND is NO_WIND then V_UAV_RE…	1	rule3
4	If R_HEL is FAR and V_R_WIND is NO_WIND then V_UAV_REL is FAST	1	rule4
5	If R_HEL is VERY_FAR and V_R_WIND is NO_WIND then V_UAV_RE…	1	rule5
6	If R_HEL is ON_TOP and Θ_R_WIND is N1 and V_R_WIND is LOW_…	1	rule6
7	If R_HEL is CLOSE and Θ_R_WIND is N1 and V_R_WIND is LOW_WI…	1	rule7
8	If R_HEL is MED_DIST and Θ_R_WIND is N1 and V_R_WIND is LOW…	1	rule8
9	If R_HEL is FAR and Θ_R_WIND is N1 and V_R_WIND is LOW_WIND …	1	rule9
10	If R_HEL is VERY_FAR and Θ_R_WIND is N1 and V_R_WIND is LOW…	1	rule10
11	If R_HEL is ON_TOP and Θ_R_WIND is NE and V_R_WIND is LOW_…	1	rule11
12	If R_HEL is CLOSE and Θ_R_WIND is NE and V_R_WIND is LOW_WI…	1	rule12
13	If R_HEL is MED_DIST and Θ_R_WIND is NE and V_R_WIND is LOW…	1	rule13
14	If R_HEL is FAR and Θ_R_WIND is NE and V_R_WIND is LOW_WIND…	1	rule14
15	If R_HEL is VERY_FAR and Θ_R_WIND is NE and V_R_WIND is LOW…	1	rule15
16	If R_HEL is ON_TOP and Θ_R_WIND is E and V_R_WIND is LOW_WI…	1	rule16
17	If R_HEL is CLOSE and Θ_R_WIND is E and V_R_WIND is LOW_WIN…	1	rule17
18	If R_HEL is MED_DIST and Θ_R_WIND is E and V_R_WIND is LOW_…	1	rule18
19	If R_HEL is FAR and Θ_R_WIND is E and V_R_WIND is LOW_WIND t…	1	rule19

The Range from the Landing Deck is shown in Table 2 below, using linguistic values: On Top (ON_TOP), Close (CLOSE), Medium Distance (MED_DIST), Far (FAR), Very Far (VERY_FAR), followed by the membership function plots of the input data (Figure 13). The RLD is calculated by the TDOA based positioning system.

Table 2: Range from the Landing Deck

Name	Type	Parameters
ON_TOP	Trapezoidal	[-18.75 -2.083 2.083 18.75]
CLOSE	Trapezoidal	[6.25 22.92 27.08 43.75]
MED_DIST	Trapezoidal	[31.25 47.92 52.08 68.75]
FAR	Trapezoidal	[56.25 72.92 77.08 93.75]
VERY_FAR	Trapezoidal	[81.25 97.92 102.1 118.7]

Figure 13: Membership Function Plot of the Range from the Landing Deck

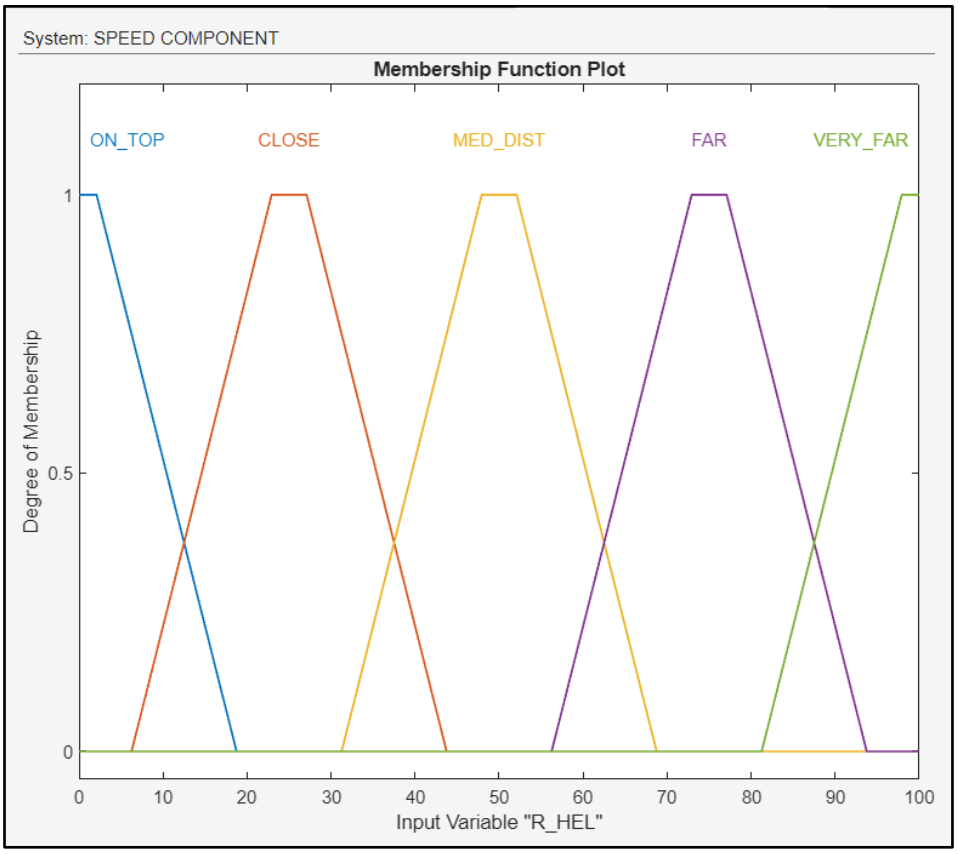

The Azimuth Angle of Wind is shown in Table 3, using the linguistic values: North (N1 and N2), North East (NE), East (E), South East (SE), South (S), South West (SW), West (W), North West (NW), followed by the membership function plots of the input data (Figure 14).

Table 3: Azimuth Angle of Wind

Name	Type	Parameters
N1	Trapezoidal	[-0.5887 -0.06542 0.065...
NE	Trapezoidal	[0.1963 0.7196 0.8504 1....
E	Trapezoidal	[0.9812 1.505 1.635 2.159]
SE	Trapezoidal	[1.766 2.29 2.42 2.944]
S	Trapezoidal	[2.551 3.075 3.205 3.729]
SW	Trapezoidal	[3.336 3.86 3.99 4.514]
W	Trapezoidal	[4.121 4.645 4.775 5.299]
NW	Trapezoidal	[4.906 5.43 5.56 6.084]
N2	Trapezoidal	[5.691 6.215 6.345 6.869]

Figure 14: Membership Function Plot of the Azimuth Angle of Wind

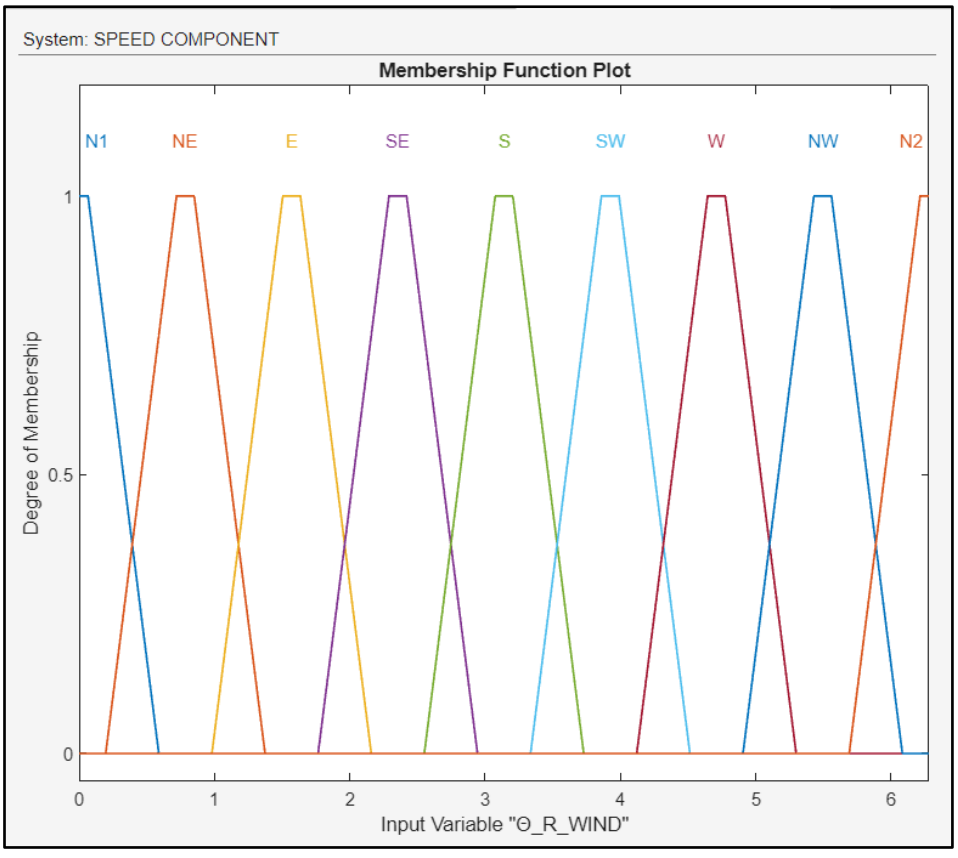

Wind Speed is shown in Table 4, using the linguistic values followed by the membership function plots of the input data (Figure 15). WS, as well as the AAW are calculated by an anemometer.

Table 4: Wind Speed

Name	Type	Parameters
NO_WIND	Trapezoidal	[-20.62 -2.292 2.292 20.62]
LOW_WIND	Trapezoidal	[6.875 25.21 29.79 48.12]
MEDIUM_WIND	Trapezoidal	[34.38 52.71 57.29 75.63]
HIGH_WIND	Trapezoidal	[61.87 80.21 84.79 103.1]
VERY_HIGH_...	Trapezoidal	[89.37 107.7 112.3 130.6]

Figure 15: Membership Function Plot of the Wind Speed

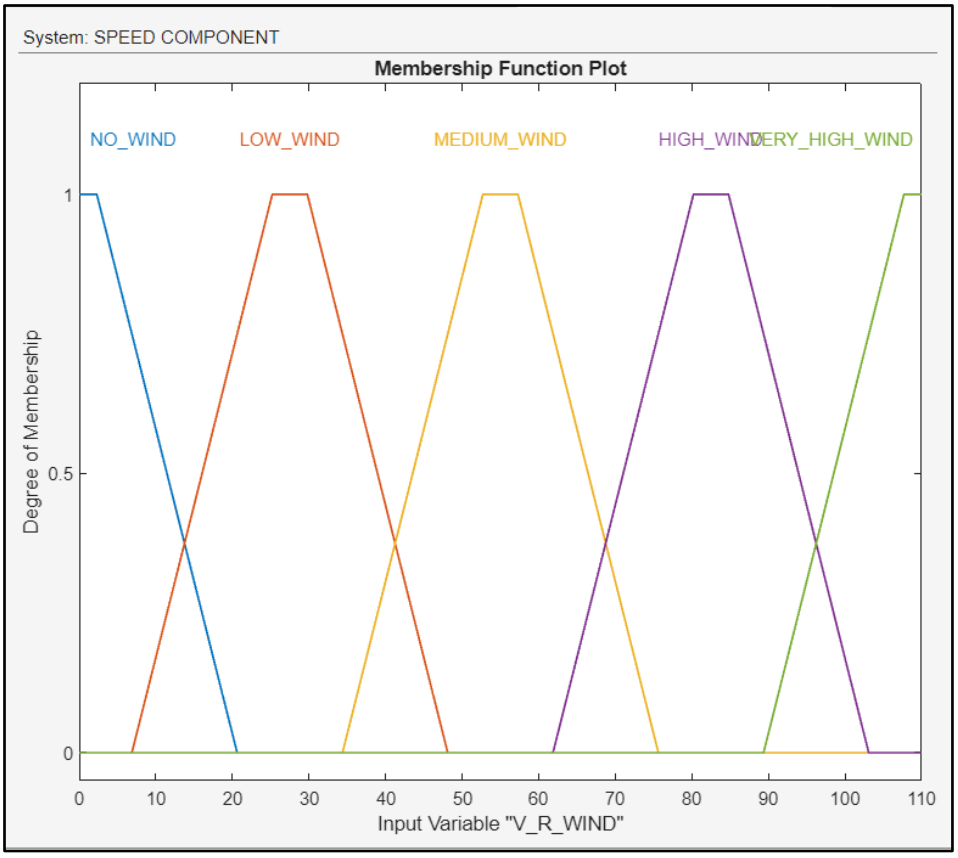

The output of the block – RSD – is shown in Table 5, using linguistic values as written below, followed by the membership function plots of the output data (Figure 16). To control the variable above, the FLS regulates the throttle of the drone.

Table 5: The Relative Speed of the UAV

Name	Type	Parameters
MIN	Trapezoidal	[-1.562 4.271 5.729 11.56]
SLOW	Trapezoidal	[7.188 13.02 14.48 20.31]
MEDIUM	Trapezoidal	[15.94 21.77 23.23 29.06]
FAST	Trapezoidal	[24.69 30.52 31.98 37.81]
MAX	Trapezoidal	[33.44 39.27 40.73 46.56]

Figure 16: Membership Function Plot of the Relative Speed

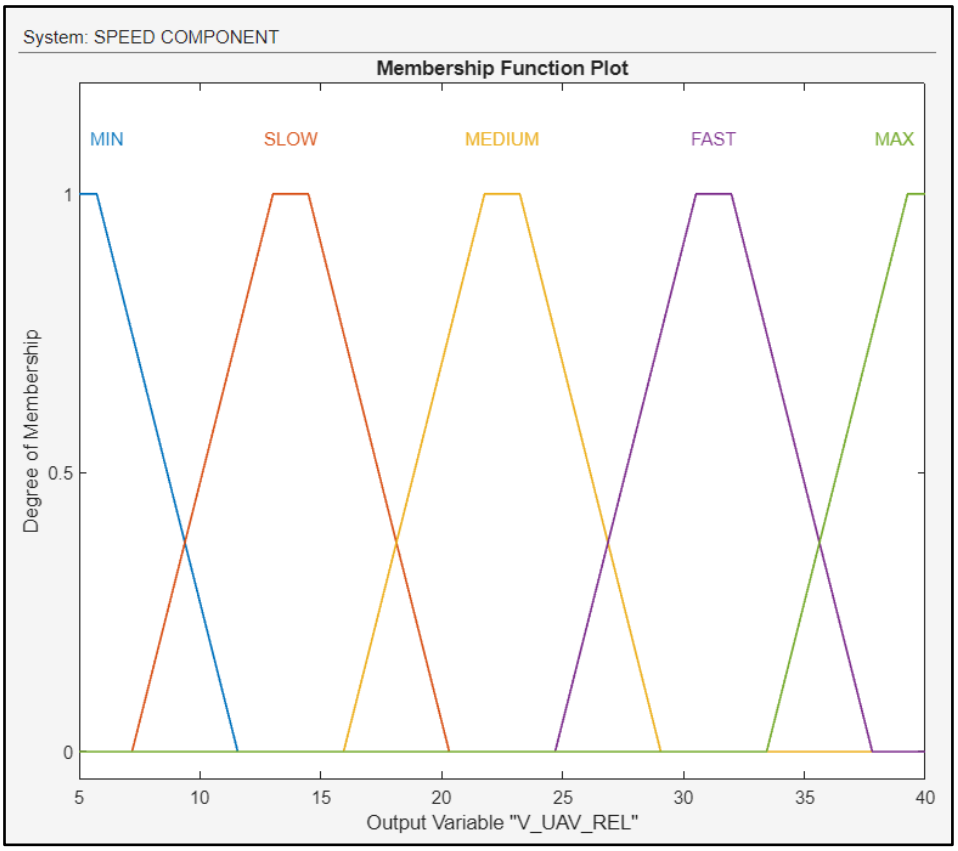

4.4.2 Lateral Motion Component

The second block is the lateral motion component, which is presented in Figure 17. The Mamdani Fuzzy Logic Component is used with three inputs: Azimuth Angle of Wind, Wind Speed and Airspeed, and one output: the Bank Angle of the UAV. The total number of rules is eighty-two (82) as shown in Figure 18.

The AAW, as well as the WS, are shown in Table 3, 4 and their membership functions in Figures 14, 15 respectively.

Figure 17: The Lateral Motion Component

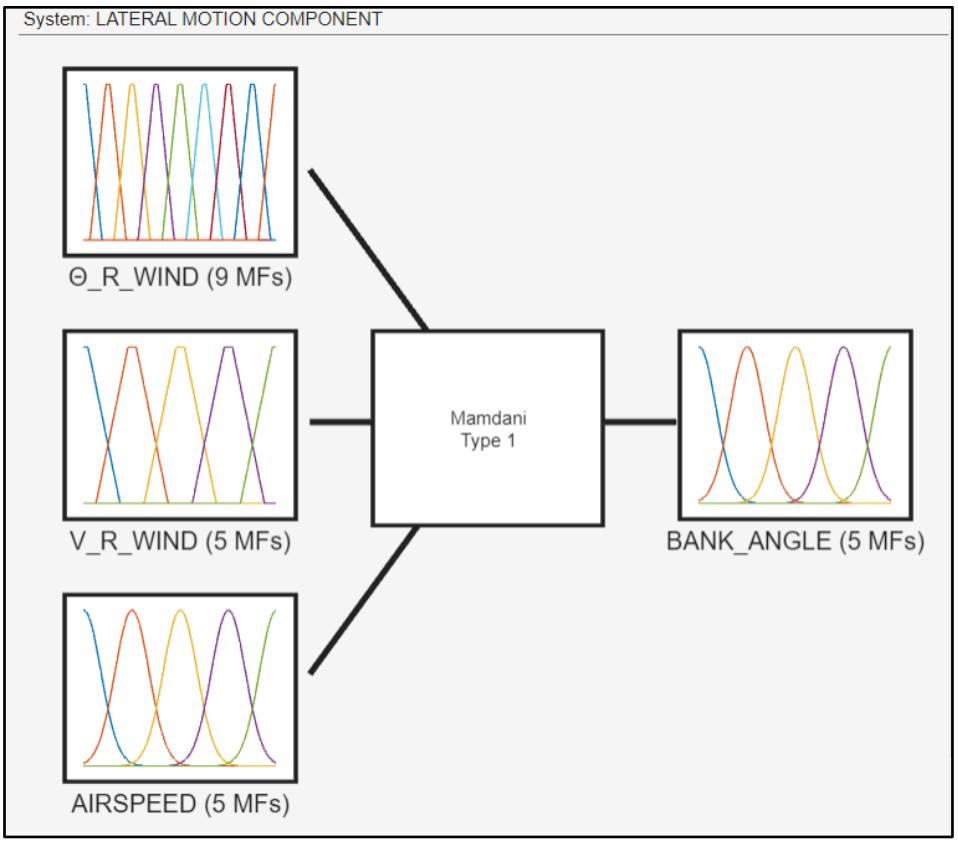

Figure 18: Rule Editor in the Lateral Motion Component

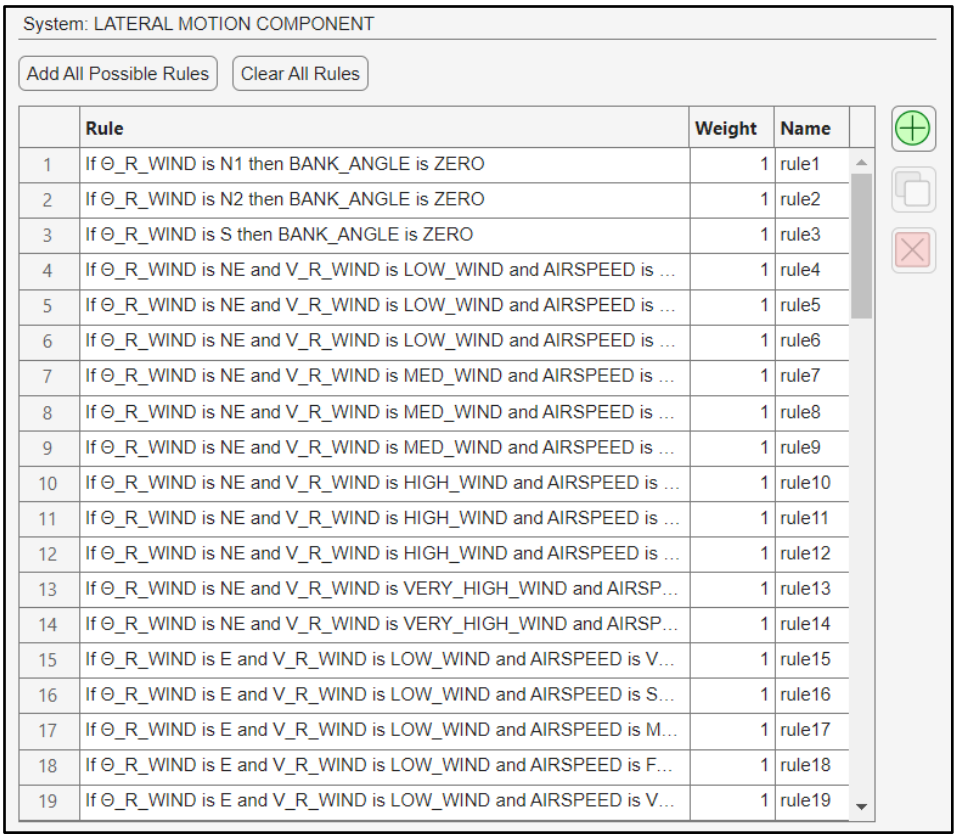

	Rule	Weight	Name
1	If Θ_R_WIND is N1 then BANK_ANGLE is ZERO	1	rule1
2	If Θ_R_WIND is N2 then BANK_ANGLE is ZERO	1	rule2
3	If Θ_R_WIND is S then BANK_ANGLE is ZERO	1	rule3
4	If Θ_R_WIND is NE and V_R_WIND is LOW_WIND and AIRSPEED is ...	1	rule4
5	If Θ_R_WIND is NE and V_R_WIND is LOW_WIND and AIRSPEED is ...	1	rule5
6	If Θ_R_WIND is NE and V_R_WIND is LOW_WIND and AIRSPEED is ...	1	rule6
7	If Θ_R_WIND is NE and V_R_WIND is MED_WIND and AIRSPEED is ...	1	rule7
8	If Θ_R_WIND is NE and V_R_WIND is MED_WIND and AIRSPEED is ...	1	rule8
9	If Θ_R_WIND is NE and V_R_WIND is MED_WIND and AIRSPEED is ...	1	rule9
10	If Θ_R_WIND is NE and V_R_WIND is HIGH_WIND and AIRSPEED is ...	1	rule10
11	If Θ_R_WIND is NE and V_R_WIND is HIGH_WIND and AIRSPEED is ...	1	rule11
12	If Θ_R_WIND is NE and V_R_WIND is HIGH_WIND and AIRSPEED is ...	1	rule12
13	If Θ_R_WIND is NE and V_R_WIND is VERY_HIGH_WIND and AIRSP...	1	rule13
14	If Θ_R_WIND is NE and V_R_WIND is VERY_HIGH_WIND and AIRSP...	1	rule14
15	If Θ_R_WIND is E and V_R_WIND is LOW_WIND and AIRSPEED is V...	1	rule15
16	If Θ_R_WIND is E and V_R_WIND is LOW_WIND and AIRSPEED is S...	1	rule16
17	If Θ_R_WIND is E and V_R_WIND is LOW_WIND and AIRSPEED is M...	1	rule17
18	If Θ_R_WIND is E and V_R_WIND is LOW_WIND and AIRSPEED is F...	1	rule18
19	If Θ_R_WIND is E and V_R_WIND is LOW_WIND and AIRSPEED is V...	1	rule19

Airspeed is shown in Table 6, using linguistic values as written below, followed by the membership function plots of the input data (Figure 19). Airspeed is calculated by an airspeed sensor.

Table 6: The Airspeed

Name	Type	Parameters
VERY_SLOW	Gaussian	[9.732 -8.882e-16]
SLOW	Gaussian	[9.732 27.5]
MEDIUM	Gaussian	[9.732 55]
FAST	Gaussian	[9.732 82.5]
VERY FAST	Gaussian	[9.732 110]

Figure 19: Membership Function Plot of the Airspeed

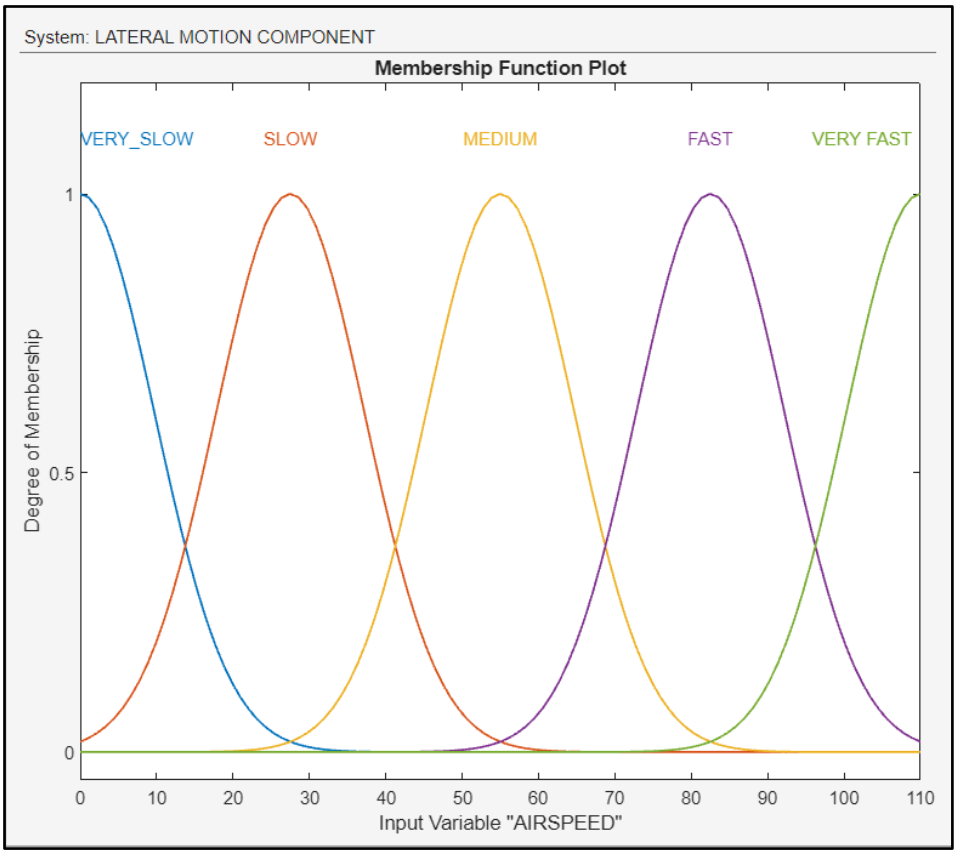

The output of the component is the Bank Angle of the UAV and is shown in Table 7, using linguistic values as written below, followed by the membership function plots of the output data (Figure 20). To control the variable above, the FLS regulates the ailerons of the drone's wings.

Table 7: The Bank Angle

Name	Type	Parameters
HARD_PORT	Gaussian	[10.62 -60]
PORT	Gaussian	[10.62 -30]
ZERO	Gaussian	[10.62 -2.22e-16]
STARBOARD	Gaussian	[10.62 30]
HARD_STARBOARD	Gaussian	[10.62 60]

Figure 20: Membership Function Plot of the Bank Angle

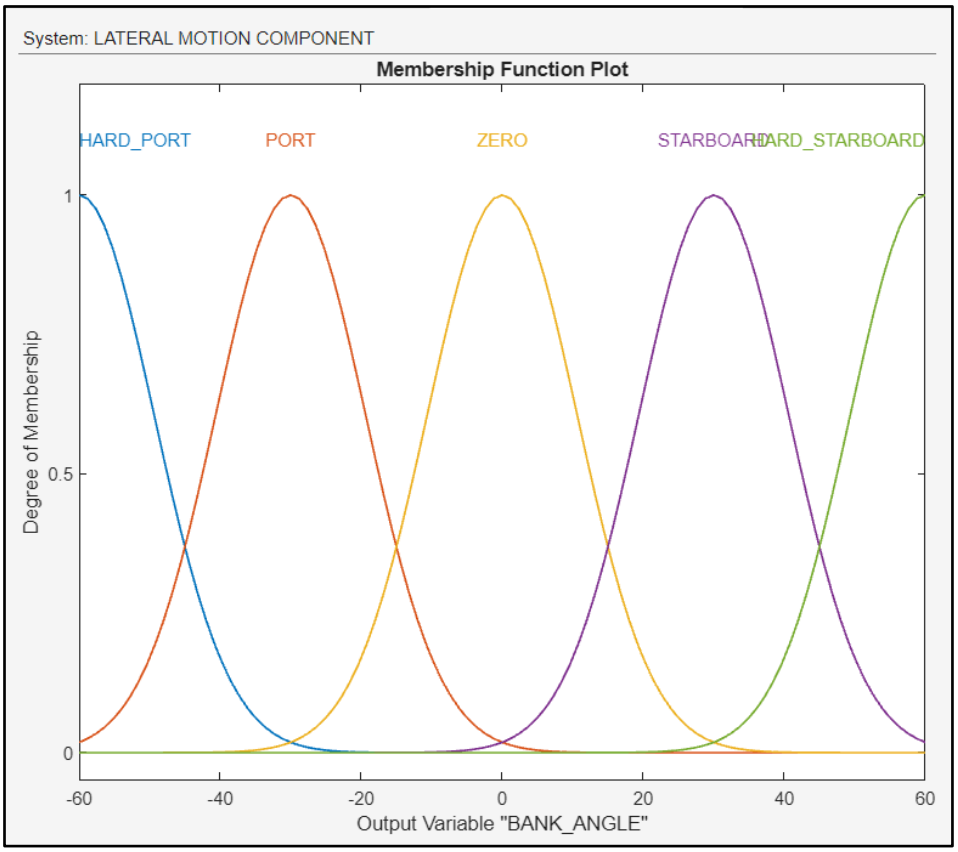

Airspeed, AAW and RWS are directly related. When the wind is stronger, then the molecules of air around the body of the vehicle will move faster, depending also on the angle that these molecules will slam the UAV's airspeed sensor. For example, if the wind is blowing against the drone's course, then the IAS will increase, as the mass of air that slams the body of the UAV will move faster.

4.4.3 Altitude Component

The third and last fuzzy logic subsystem block is the altitude component, which is presented in Figure 21. The Mamdani Fuzzy Logic Component is used with three inputs: Range from Landing Deck, Altitude and Airspeed, and one output: the AOD of the UAV. The total number of rules is one hundred and five (105) as shown in Figure 22.

The Range from Landing Deck, as well as the Airspeed, are shown in Table 2, 6 and their membership functions in Figures 13, 19 respectively.

Figure 21: The Altitude Component

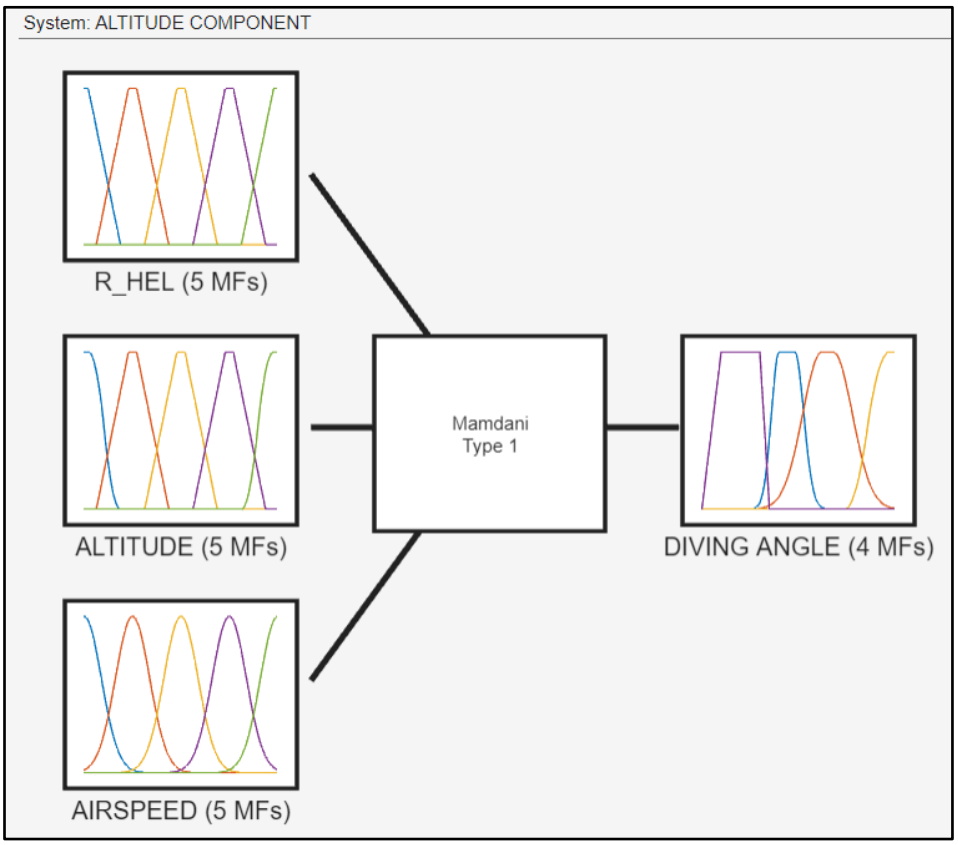

Figure 22: Rule Editor in the Altitude Component

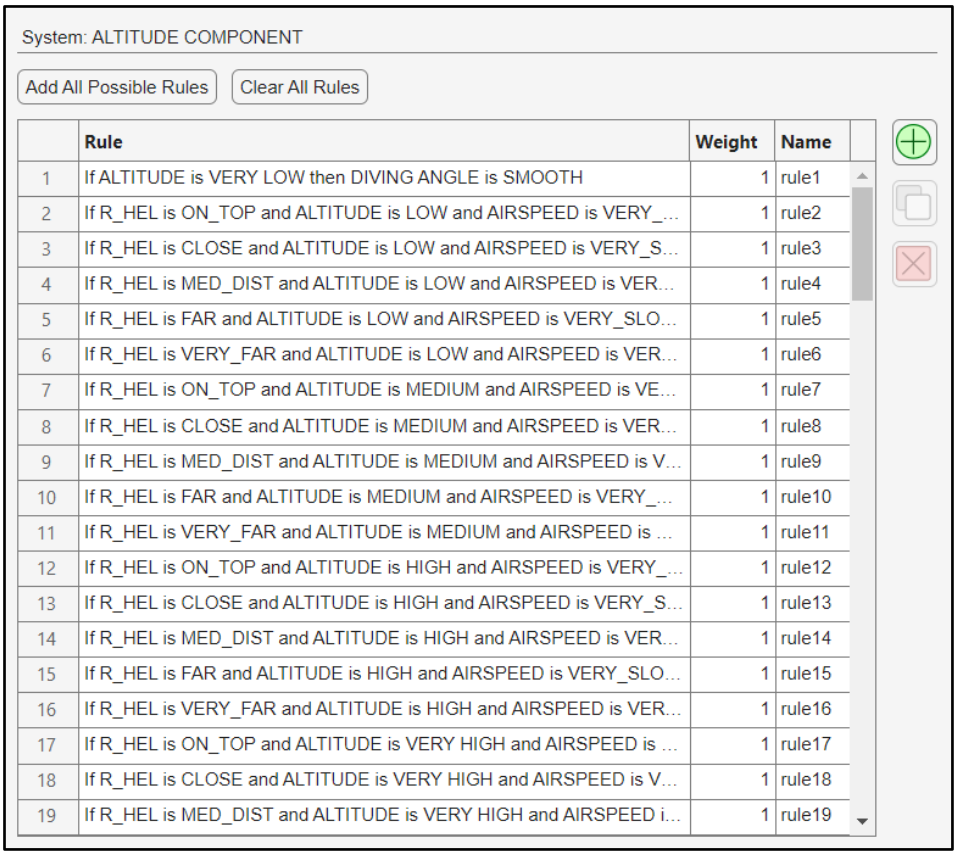

	Rule	Weight	Name
1	If ALTITUDE is VERY LOW then DIVING ANGLE is SMOOTH	1	rule1
2	If R_HEL is ON_TOP and ALTITUDE is LOW and AIRSPEED is VERY_...	1	rule2
3	If R_HEL is CLOSE and ALTITUDE is LOW and AIRSPEED is VERY_S...	1	rule3
4	If R_HEL is MED_DIST and ALTITUDE is LOW and AIRSPEED is VER...	1	rule4
5	If R_HEL is FAR and ALTITUDE is LOW and AIRSPEED is VERY_SLO...	1	rule5
6	If R_HEL is VERY_FAR and ALTITUDE is LOW and AIRSPEED is VER...	1	rule6
7	If R_HEL is ON_TOP and ALTITUDE is MEDIUM and AIRSPEED is VE...	1	rule7
8	If R_HEL is CLOSE and ALTITUDE is MEDIUM and AIRSPEED is VER...	1	rule8
9	If R_HEL is MED_DIST and ALTITUDE is MEDIUM and AIRSPEED is V...	1	rule9
10	If R_HEL is FAR and ALTITUDE is MEDIUM and AIRSPEED is VERY_...	1	rule10
11	If R_HEL is VERY_FAR and ALTITUDE is MEDIUM and AIRSPEED is ...	1	rule11
12	If R_HEL is ON_TOP and ALTITUDE is HIGH and AIRSPEED is VERY_...	1	rule12
13	If R_HEL is CLOSE and ALTITUDE is HIGH and AIRSPEED is VERY_S...	1	rule13
14	If R_HEL is MED_DIST and ALTITUDE is HIGH and AIRSPEED is VER...	1	rule14
15	If R_HEL is FAR and ALTITUDE is HIGH and AIRSPEED is VERY_SLO...	1	rule15
16	If R_HEL is VERY_FAR and ALTITUDE is HIGH and AIRSPEED is VER...	1	rule16
17	If R_HEL is ON_TOP and ALTITUDE is VERY HIGH and AIRSPEED is ...	1	rule17
18	If R_HEL is CLOSE and ALTITUDE is VERY HIGH and AIRSPEED is V...	1	rule18
19	If R_HEL is MED_DIST and ALTITUDE is VERY HIGH and AIRSPEED i...	1	rule19

Altitude is shown in Table 8, using linguistic values as written below, followed by the membership function plots of the input data (Figure 23). Altitude is calculated by a barometric altimeter, combined with the 3D TDOA based localization system.

Table 8: The Altitude

Name	Type	Parameters
VERY LOW	Z-shaped	[18.62 71.62]
LOW	Trapezoidal	[31.88 84.88 98.12 151.1]
MEDIUM	Trapezoidal	[111.4 164.4 177.6 230.6]
HIGH	Trapezoidal	[190.9 243.9 257.1 310.1]
VERY HIGH	S-shaped	[270.4 323.4]

Figure 23: Membership Function Plot of the Altitude

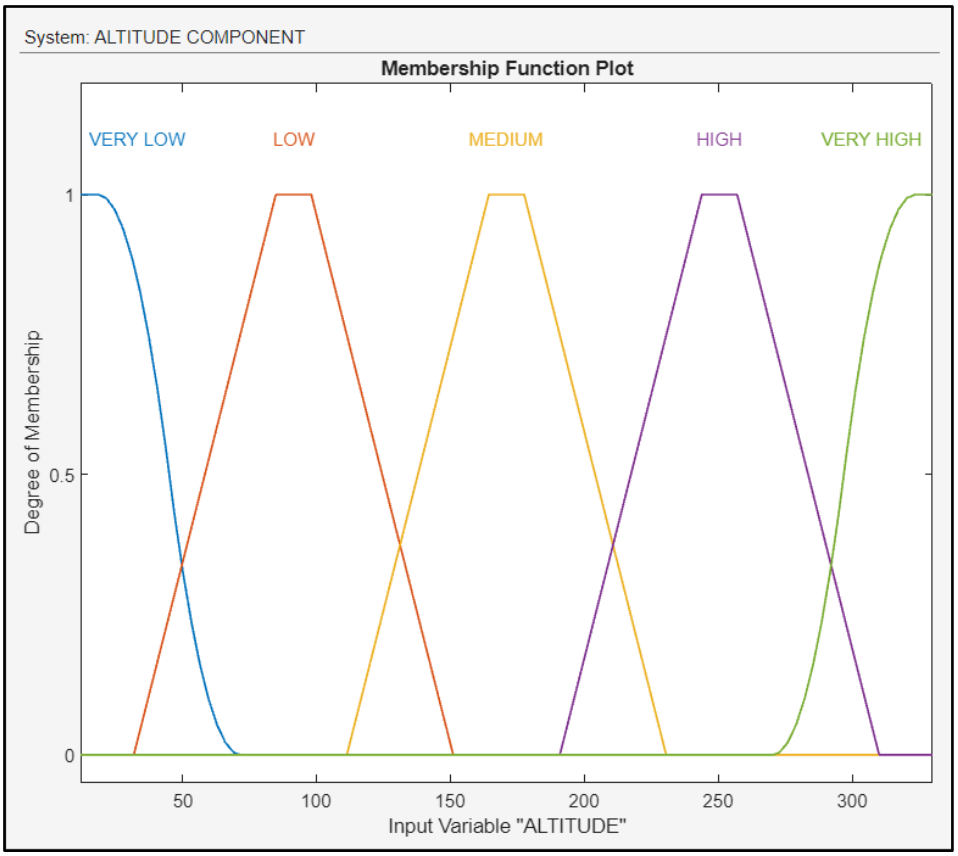

The output of the component is the AOD of the UAV and is shown in Table 9, using linguistic values as written below, followed by the membership function plots of the output data. To control the variable above, the FLS regulates both the ailerons of the drone's wings, either up or down.

Table 9: The Angle Of Descent

Name	Type	Parameters
SMOOTH	Two-sided Gauss...	[0.4 1 0.4728 1.8]
MEDIUM	Two-sided Gauss...	[0.9909 3.208 0.9909 3.7...
STEEP	S-shaped	[4.375 6.708]
ABORT	Trapezoidal	[-3 -2 0 0.5]

Figure 24: Membership Function Plot of the Angle Of Descent (Diving Angle)

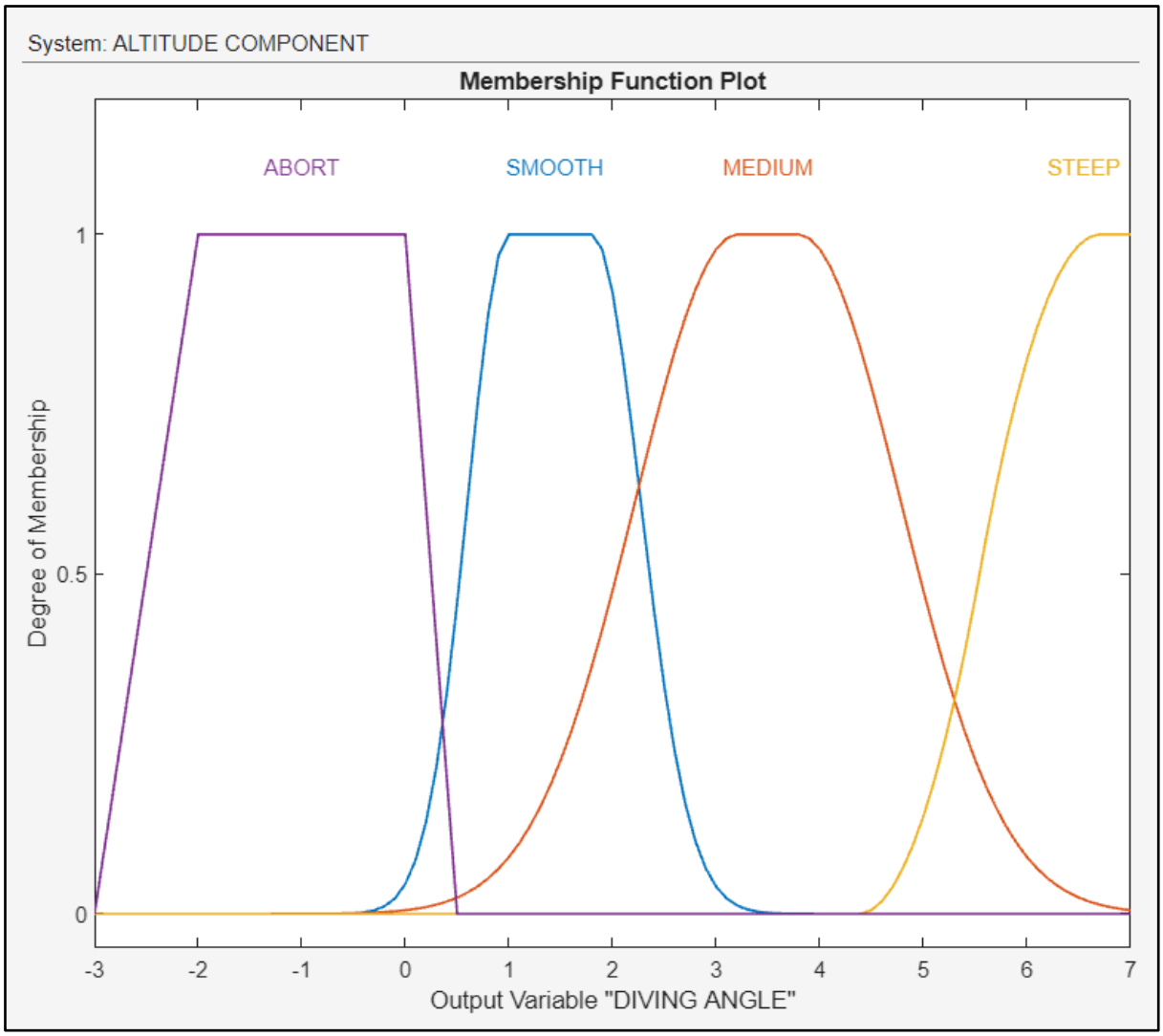

The vertical control and airspeed of a UAV exhibit a reciprocal relationship—when the UAV pitches upward, its speed decreases proportionally, and conversely, pitching downward leads to an increase in speed [4]. Notably, in this study, it is considered that there is no interdependency between airspeed and vertical control.

4.5 Landing Simulation Results

With the FLS now prepared, it's time to input crisp values into the Rule Viewer's input field to commence the simulation. The Rule Inference of every component, based upon the input and output parameters, as well as the fuzzy rules that were implemented previously, calculates the desired output value of the subsystem block. For each component an example is presented in the Rule Inference tab and afterwards, the Control Surfaces are shown for each pair of inputs, in order to understand the relations between two of the inputs compared to the output value of every block.

4.5.1 Speed Component Results

As presented in the figure below (Figure 25), in the case of a UAV at a distance of *27 meters* from the landing deck, with winds blowing from *1.88 rads* (approximately *107 degrees*) at a speed of *40 knots*, the required RSD in relation to the ship's velocity will be *12.8 knots* in order to land effectively onboard the ship. To obtain a different result, entering new values into the input field is necessary [22].

Figure 25: Rule Inference for the Speed Component

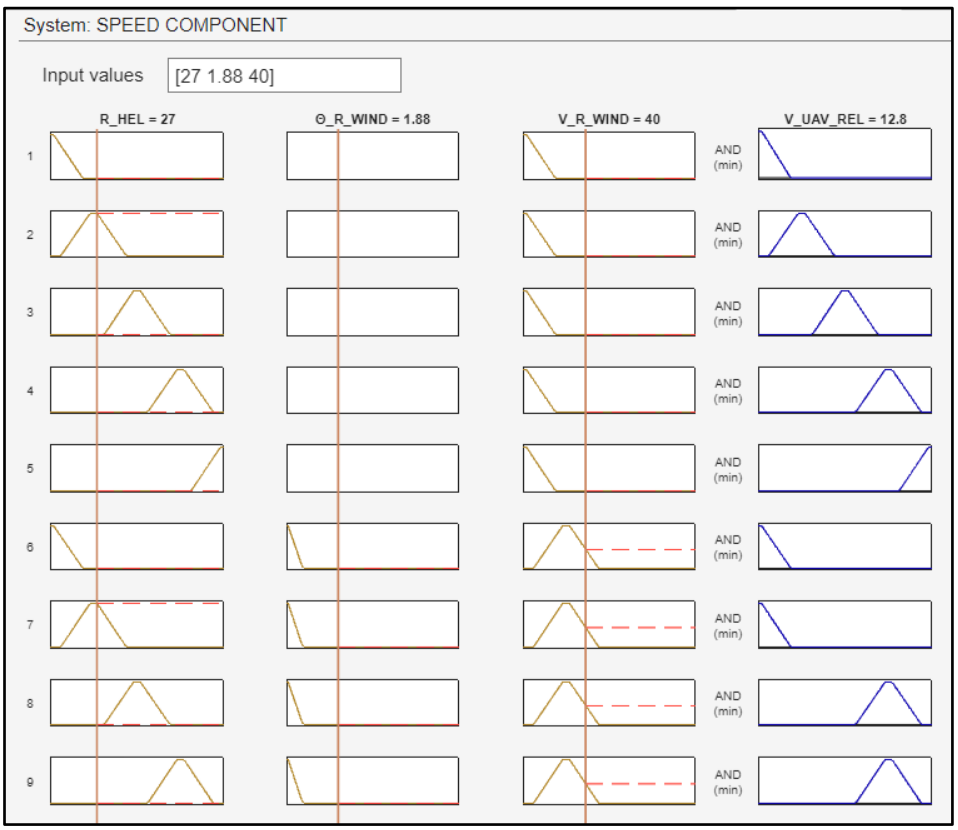

Figure 26 below shows the surface of Relative UAV Speed as the dependency between Relative Wind Speed for various Ranges from the Landing Deck.

Figure 26: Relative UAV Speed in relations with Range from the Landing Deck and Relative Wind Speed

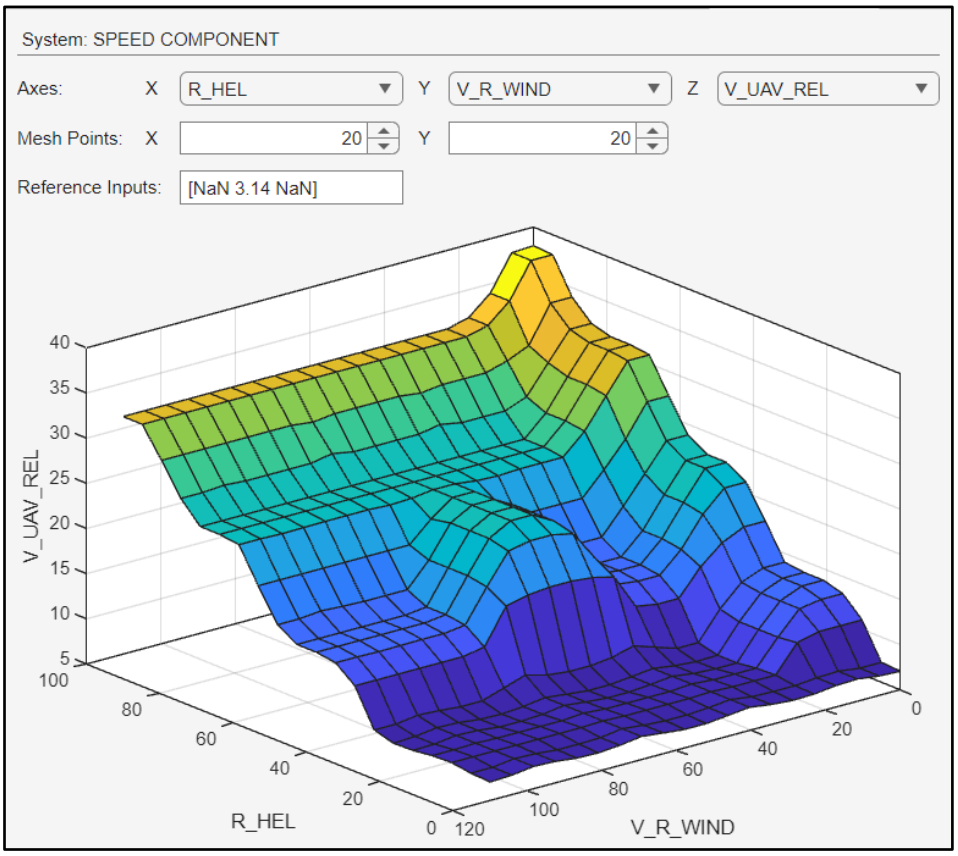

Figure 27 illustrates the surface of Relative UAV Speed, on the x axis is shown the AAW in rads and on the y axis is the Relative Wind Speed.

Figure 27: Relative UAV Speed in relations with Azimuth Angle of Wind and Relative Wind Speed

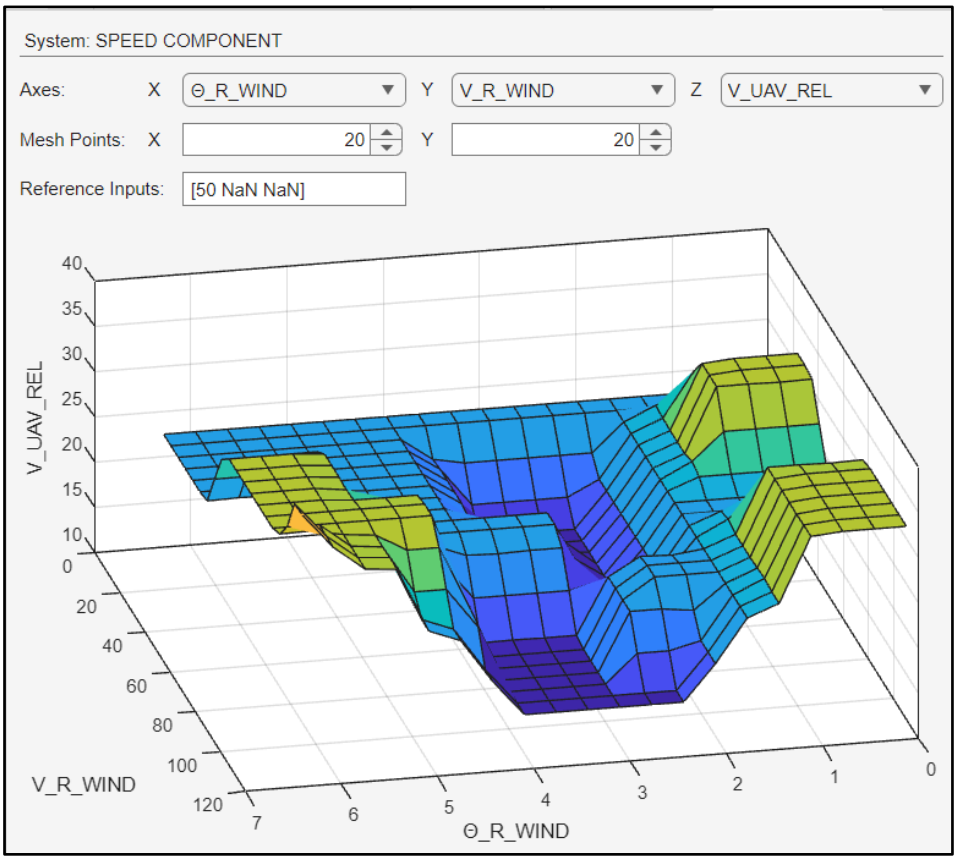

4.5.2 Lateral Motion Component Results

Figure 28, illustrates the case of a UAV flying with an IAS of *70 knots*, with winds blowing from *1.88 rads* (approximately *107 degrees*) at a RSD of *40 knots*. As a result, during the turn that the UAV will make to correct its course, a BA of *36.3 degrees* will be executed.

Figure 28: Rule Inference for the Lateral Motion Component

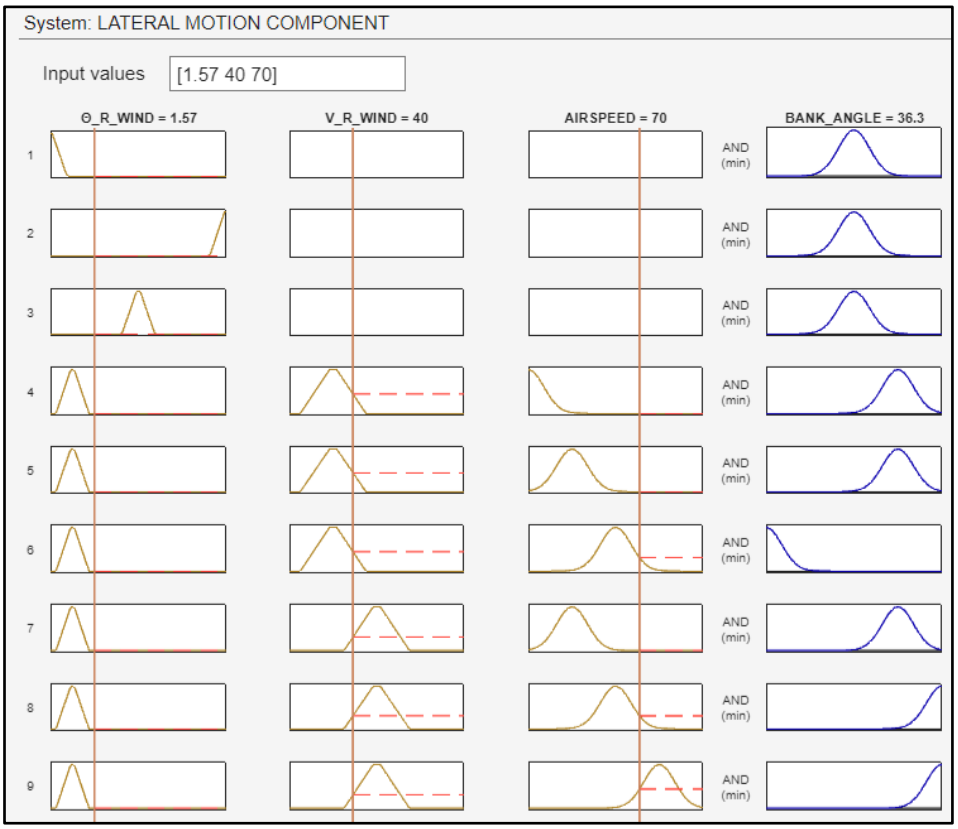

In Figure 29, the surface of BA as the dependency between AAW for different values of airspeed.

Figure 29: Bank Angle in relations with Azimuth Angle of Wind and Airspeed

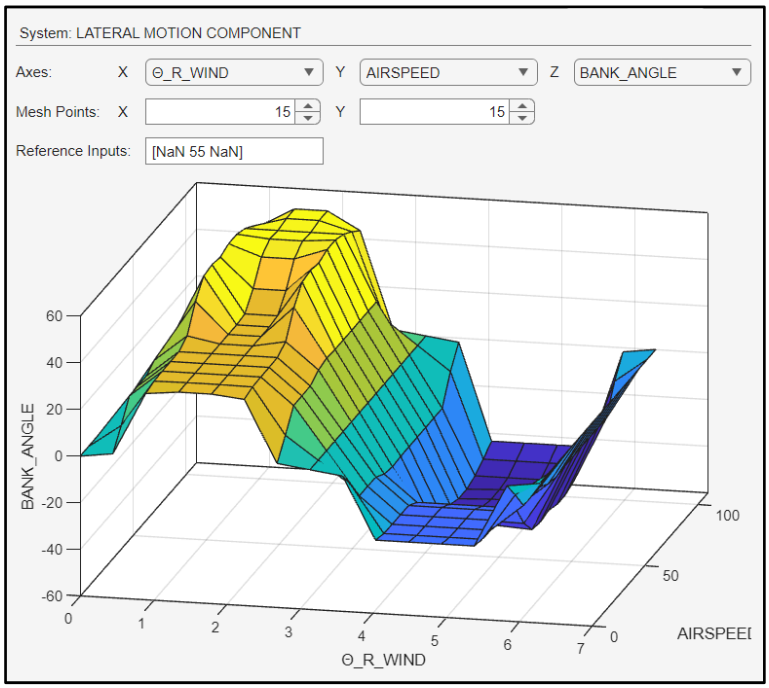

Figure 30 illustrates the surface of Bank Angle, on the x axis is shown the AAW in rads and on the y axis is the RWS.

Figure 30: Bank Angle in relations with Azimuth Angle of Wind and Relative Wind Speed

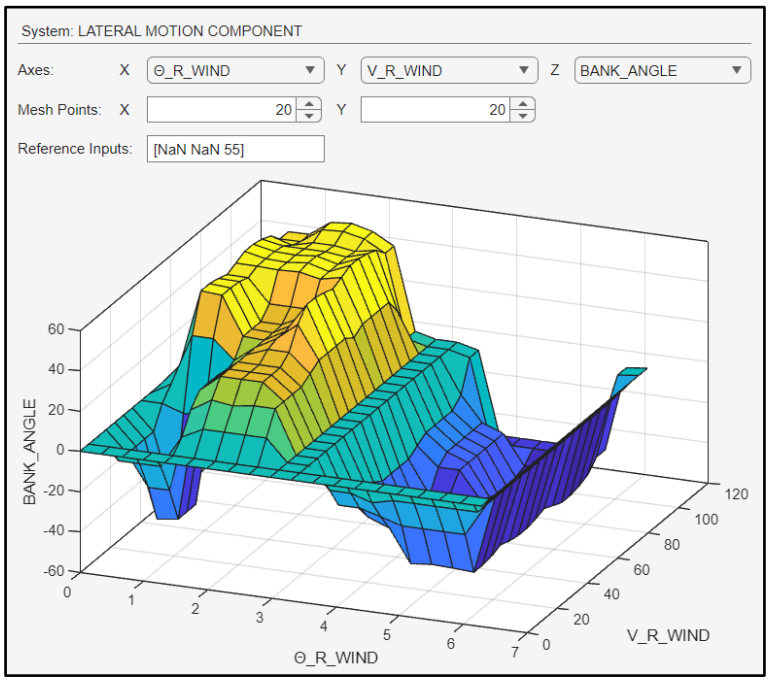

4.5.3 Altitude Component

In Figure 31, the UAV flies with an IAS of *70 knots*, at a range of *27m* from the landing deck, at a height level (altitude) of *120 feet*. Consequently, the AOD of the UAV is set to 3.22 degrees, ensuring a sufficient altitude for a successful landing on the "SkyHook" capture system.

Figure 31: Rule Inference for the Altitude Component

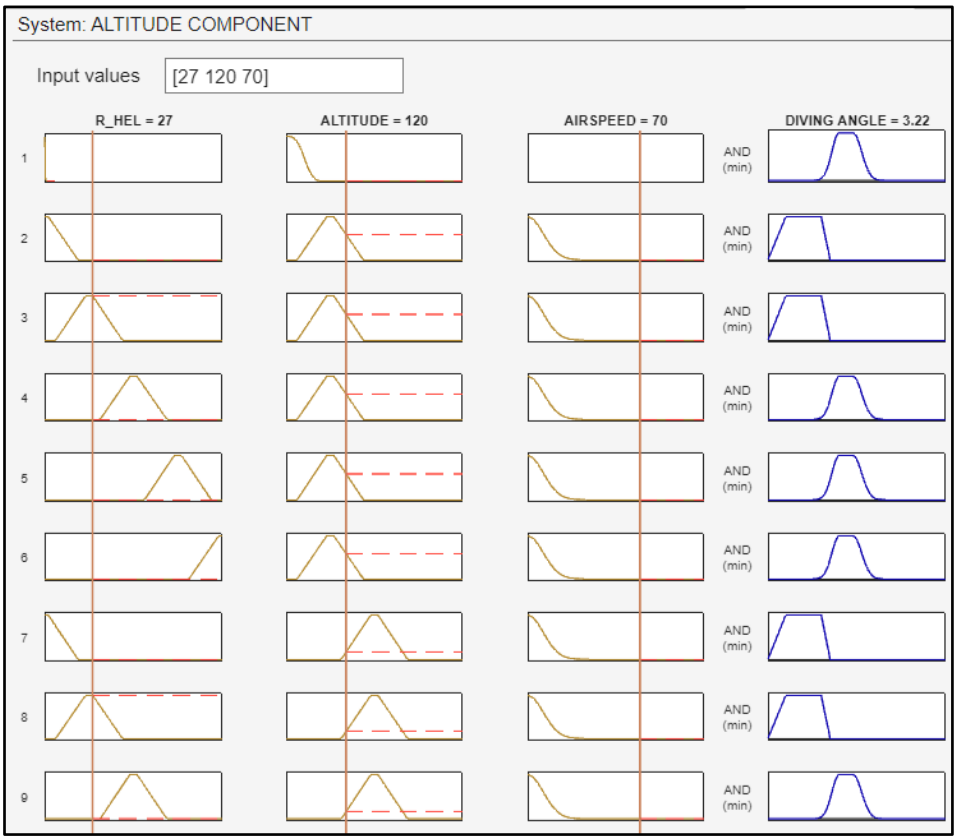

Figure 32 illustrates the surface of the Angle of Descent, on the x axis the Range from the Landing Deck is shown (in meters) and on the y axis is the Airspeed (in knots).

Figure 32: Angle of Descent (Diving Angle) in relations with Range from the Landing Deck and Airspeed

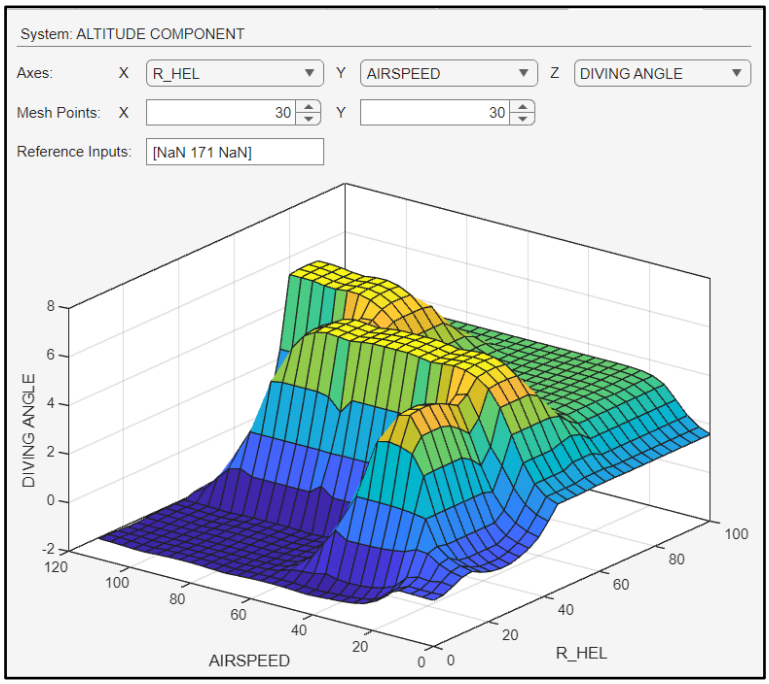

Figure 33 below illustrates again the surface of the Angle of Descent, however on the x axis the Range from the Landing Deck is shown (in meters) and on the y axis is the Altitude.

Figure 33: Angle of Descent (Diving Angle) in relations with Range from the Landing Deck and Altitude

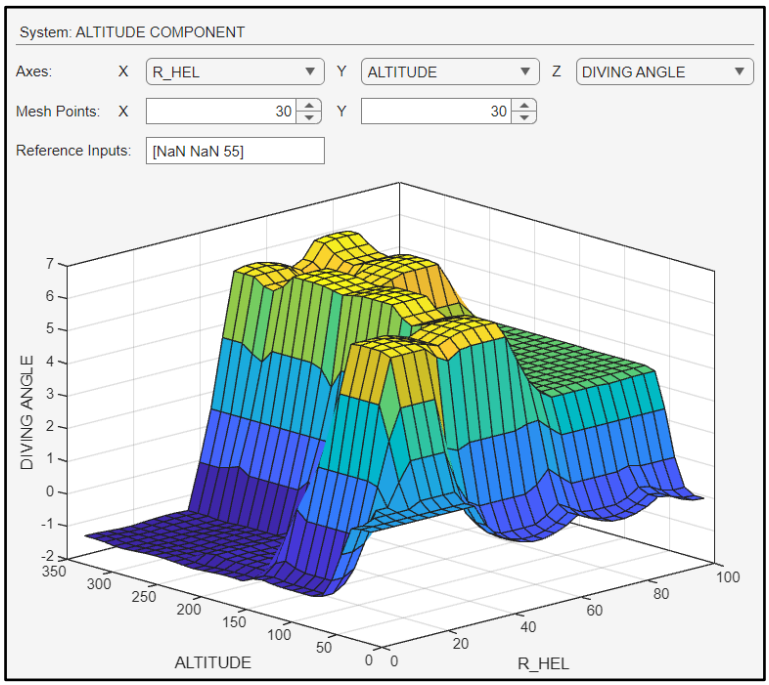

In conclusion, in the case of a UAV operating at a distance of *27 meters* from the landing deck, at an altitude of *120 feet*, with winds blowing from *1.88 rads* (approximately *107 degrees*) at a speed of *40 knots* and an IAS of *70 knots*, the required RSD in relation to the ship's velocity will be *12.8 knots*, during the turn that will be executed the UAV will have a BA of *36.3 degrees* and the AOD will have a value of *3.22* degrees.

4.5.4 Simulated Outcomes of the FLS

To test the reliability and effectiveness of the FLS, a certain number of different input values was imported in the rule inference tab of the FuzzyLogicDesigner Toolbox in MATLAB software. The output results are shown in Table 10.

Table 10: Input-Output Data

S/N	INPUTS					OUTPUTS		
	RLD	AAW	RWS	IAS	ALTITUDE	RSD	BA	AOD
1.	08	355	41	52	45	13.3	-2.37×10^{-16}	1.77
2.	14	220	12	26	96	12.6	-11.7	2.18
3.	27	166	24	31	235	7.36	4.57	6.15
4.	34	096	35	58	179	15.9	30	5.25
5.	45	035	25	19	192	31.3	29.8	3.38
6.	51	015	98	105	211	31.2	6.14	4.57
7.	66	275	46	63	23	29.1	-50.7	2.02
8.	75	197	08	44	79	30.4	-3.52	0.7
9.	82	306	17	28	56	31.4	-21.1	1.84
10.	96	340	10	12	13	37.6	-8.7	2.42

5. Conclusion and Future Suggestions

The primary aim of this research is to design a fuzzy logic-based autonomous ship-deck landing system specifically tailored for medium/small class fixed-wing UAVs. This system aims to alleviate maritime UAV operators from the demanding and challenging task of landing a drone on a moving ship. A variety of sensors onboard the UAV and also onboard the ship has been utilized, including RF localization systems such as RFID and TDOA based mechanisms, anemometers, altimeters and airspeed sensors. However, a key objective of this study is to reduce the requisite number of sensors and equipment, with a dual focus on cost-effectiveness and diminished system complexity. Additionally, particular attention has been given to the deliberate exclusion of GPS, enhancing the UAV's resistance to long range EW jamming and spoofing techniques.

The purpose of the autonomous ship-deck landing system is to control the UAV's movement in the three-dimensional space, ensuring precise positional control during the final approach. The wind, being an external factor that directly influences drone landing, particularly at sea, is integrated into the fuzzy logic-based system along with the airspeed of the UAV, altitude, and the distance from the landing platform. This integration is facilitated through the UAV's sensors. The FLS in return, provides as outputs: the RSD in relation with the speed of the ship, the angle of descent and the bank angle of the drone, or else the azimuth angle of turn, in order to control the UAV's movement. The membership functions utilized in the FLS, as well as its associated rule base, are determined heuristically. However, the simulation results are generally satisfactory, affirming the reliability of the autonomous fuzzy logic landing system.

Lastly, future suggestions would involve searching for more optimal membership function parameters and rule base, by incorporating the knowledge and the experience of maritime UAV operators, in combination with those of maritime helicopter pilots, who undeniably excel in harsh, all-weather landings onboard ships, utilizing polls or other statistic methods. Research could also explore additional input variables or parameters, such as humidity or visibility (particularly relevant when utilizing computer vision algorithms for landing). These factors significantly impact UAV navigation and control during the final stage of flight, where environmental conditions and the drone's aerodynamics differ significantly from the usual phases of UAV flight.

Bibliography

[1] A. Krystosik-Gromadzińska, "The use of drones in the maritime sector – areas and benefits," Scientific Journals of the Maritime University of Szczecin, Szczecin, Poland, 2021.

[2] M. Chukwube, "The Role of UAVs in Border Security and Maritime Surveillance," readwrite, 3 April 2023. [Online]. Available: https://readwrite.com/the-role-of-uavs-in-border-security-and-maritime-surveillance/.

[3] Flyability, "WHAT IS A MARITIME DRONE?," Flyability, [Online]. Available: https://www.flyability.com/maritime-drone.

[4] O. Cetin, S. Kurnaz and O. Kaynak, "Fuzzy Logic Based Approach to Design of Autonomous Landing System for Unmanned Aerial Vehicles," Istanbul, 2010.

[5] K. P. Valavanis and G. J. Vachtsevanos, "Handbook of Unmanned Aerial Vehicles," 2014.

[6] J. Sieger, "Electronic warfare: Israel ramps up GPS jamming to counter Hamas drone attacks," FRANCE 24, 17 October 2023. [Online]. Available: https://www.france24.com/en/tv-shows/science/20231017-electronic-warfare-israel-ramps-up-gps-jamming-to-counter-hamas-drone-attacks.

[7] . P. Mozur and A. Krolik, "The Invisible War in Ukraine Being Fought Over Radio Waves," The New York Times, 19 November 2023. [Online]. Available: https://www.nytimes.com/2023/11/19/technology/russia-ukraine-electronic-warfare-drone-signals.html.

[8] SKYbrary, "SKYbrary," 2021. [Online]. Available: https://skybrary.aero/articles/air-speed-indicator.

[9] IVAO Documentation Library, "IVAO Documentation Library," 29 April 2023. [Online]. Available: https://wiki.ivao.aero/en/home/training/documentation/Airspeed_definition.

[10] NWCG National Wildfire Coordinating Group, "NWCG National Wildfire Coordinating Group," [Online]. Available: https://www.nwcg.gov/course/ffm/location/62-azimuths#:~:text=However%2C%20plots%20of%20wind%20and,the%20southeast%20(135%C2%B0)..

[11] Barcelona Field Studies Center, Google Maps Compass Application, "Set Compass," [Online]. Available: https://setcompass.com/TypesofNorth.htm.

[12] R. F. Wijaya , Y. M. Tondang and A. P. Utama Siahaan, "Take Off and Landing Prediction Using Fuzzy Logic," International Journal of Recent Trends in Engineering and Research, Sumatera Utara, Indonesia, 2016.

[13] RYA Training Center, "Jolly Parrot Sailing," [Online]. Available: https://jollyparrot.co.uk/blog/the-difference-between-true-and-apparent-wind-speed-480#:~:text=True%20wind%20speed%2C%20sometimes%20known,on%20you%20as%20you%20sail..

[14] Anritsu Advancing Beyond, "Time Difference of Arrival (TDOA)," Anritsu Americas Sales Company, Allen, USA, 2022.

[15] B. Yang and E. Yang, "A Survey on Radio Frequency based Precise Localisation Technology for UAV in GPS-denied Environment," *Springer: Journal of Intelligent & Robotic Systems (2021) ,* p. 30, 6 October 2021.

[16] B. O'Keefe, "Techniques, Finding Location with Time of Arrival and Time Difference of Arrival," Department of Electrical and Computer Engineering, 2017.

[17] K. Dogancay and H. Hmam, "3D TDOA Emitter Localization Using Conic Approximation," *MDPI Sensors 2023,* p. 15, 9 July 2023.

[18] J. N. Ostler, W. J. Bowman, D. O. Snyder and T. W. McLain, "Performance Flight Testing of Small Electric Powered Unmanned Aerial Vehicles," BYU ScholarsArchive, Brigham Young University, 2009.

[19] AGENCIA NACIONAL DE AVIACAO CIVIL, "ANACPEDIA," [Online]. Available: https://www2.anac.gov.br/anacpedia/ing-por/tr686.htm#:~:text=to%3A%20%22B%22-,bank%20angle,starboard%20(left%20or%20right)..

[20] PowerNationTV, "PowerNationTV," 3 May 2017. [Online]. Available: https://www.powernationtv.com/post/how-to-land-a-drone-aircraft-with-no-runway-the-skyhook-recovery-system.

[21] MathWorks, "Object Tracking Using Time Difference of Arrival (TDOA)," MathWorks, 2021. [Online]. Available: https://www.mathworks.com/help/fusion/ug/object-tracking-using-time-difference-of-arrival.html.

[22] T. Iizuka, T. Sasatani, T. Nakamura, N. Kosaka, M. Hisada and Y. Kawahara, "MilliSign: mmWave-Based Passive Signs for Guiding UAVs in Poor Visibility Conditions," ACM MobiCom '23, Tokyo, Japan, 2023.

[23] L. L. L. McLauchlan, "Fuzzy Logic Controlled Landing of a Boeing 747," International Conference on Intelligent Robots and Systems, St. Louis, USA, 2009.

[24] W. Pratiwi, A. Sofwan and . I. Setiawan, "Implementation of fuzzy logic method for automation of decision making of Boeing aircraft landing," IAES International Journal of Artificial Intelligence (IJ-AI), Diponegoro University, Indonesia, 2020.

[25] Z. Y. Seitbattalov, S. K. Atanov and Z. S. Moldabayeva, "An Intelligent Decision Support System for Aircraft Landing Based on the Runway Surface," IEEE Smart Information Systems and Technologies (SIST), Nur-Sultan, Kazakhstan, 2021.

[26] SENSOR PARTNERS, "SENSOR PARTNERS," [Online]. Available: https://sensorpartners.com/en/knowledge-base/the-different-types-of-laser-sensors/#:~:text=Laser%20distance%20sensors%20measure%20distances,receives%20the%20reflection%20from%20it..

[27] Stanford Encyclopedia of Philosophy, "Fuzzy Logic," Stanford Encyclopedia of Philosophy, 15 November 2016. [Online]. Available: https://plato.stanford.edu/entries/logic-fuzzy/.